Dalton Transactions

PAPER

View Article Online
View Journal | View Issue

Cite this: *Dalton Trans.*, 2014, **43**, 6786

Versatile reactivity of a rhodium(I) boryl complex towards ketones and imines†

Sabrina I. Kalläne, Thomas Braun,* Beatrice Braun and Stefan Mebs

Received 9th January 2014,
Accepted 17th February 2014

DOI: 10.1039/c4dt00080c

www.rsc.org/dalton

The rhodium(I) boryl complex [Rh(Bpin)(PEt_3)$_3$] (**1**) reacts with the ketones α,α,α-trifluoroacetophenone and 9-fluorenone by insertion of the C=O bond to give [Rh{η^3-C(CF_3)(OBpin)C_6H_5}(PEt_3)$_2$] (**4**) and [Rh{η^5-$C_{13}H_8$(OBpin)}(PEt_3)$_2$] (**6**), whereas the reaction with acetophenone leads to the formation of [Rh(H)(PEt_3)$_3$] (**2**), [Rh(OBpin)(PEt_3)$_3$] (**3**) and (*E*)-(Ph)CH=CHBpin. Treatment of **1** with ketimines generates [Rh{η^3-C_6H_5=C(Ph)N(Ph)(Bpin)}(PEt_3)$_2$] (**7**), [Rh{(η^3-$C_{12}H_8$)N(Ph)(Bpin)}(PEt_3)$_2$] (**8**) or [Rh{CPh_2N(H)(Bpin)}-(PEt_3)$_2$] (**9**). The insertion of aldimines into the Rh–B bond gives access to [Rh[η^3-CH{N(C_6H_{13})Bpin}-C_6H_5](PEt_3)$_2$] (**11**) or [Rh[η^3-CH{N(Ph)Bpin}C_6H_5](PEt_3)$_2$] (**12**). The latter is converted into the C–H activation product [Rh{(C_6H_4)-*o*-N(Bpin)(CH_2Ph)}(PEt_3)$_3$] (**13**). Complex **13** reacts with B_2pin_2 to yield the boryl complex **1** and the amine $PhCH_2$N(Bpin)(C_6H_4-*o*-Bpin).

Introduction

Transition metal boryl complexes[1–6] have received considerable attention due to their role as key intermediates in metal-catalyzed borylation reactions to generate borylated derivatives.[7–12] Rhodium boryl complexes[13] are known to enable catalytic processes such as the hydroboration and dehydrogenative borylation of olefins,[14–22] the diboration of alkenes and alkynes[23,24] or the functionalization of hydrocarbons *via* C–H activation reactions.[10,12,25–31]

Many examples of the metal-catalyzed diboration of alkenes and alkynes using diboranes have been reported,[8] particularly employing Rh (for the alkenes)[32–35] and Pt complexes (in both cases). In certain circumstances the reaction also proceeds in the presence of Lewis-bases[36] or without a catalyst. Methods for the 1,2-diboration of carbon–heteroatom double bonds are rare, although such a conversion would for instance represent a direct pathway to a variety of α-functionalized boronate esters,[37,38] which are useful building blocks[39,40] and some of which have pharmaceutical applications.[40,41] In most of the cases the reaction of diboranes with heteroatom-containing, unsaturated organics are not selective and give a variety of products.

Baker and Westcott have reported the rhodium-catalyzed diboration of a thioketone by selective addition of B_2cat_2 (cat = catecholato) to thiocamphor.[37,42] In 2000, Baker *et al.* also achieved the catalytic diboration of C=N bonds to synthesize α-amino boronates with [Pt(cod)$(Cl)_2$] (cod = 1,5-cyclooctadiene) as a catalyst.[43] The synthetic potential is limited by the substrates: good results were only obtained by treatment of aldimines of the type ArCH=NR bearing a sterically bulky *N*-aryl group (R) or *ortho* directing groups at the *C*-aryl substituents (Ar) and by using B_2cat_2. The authors observed no reaction by using the same catalyst, but B_2pin_2 (pin = pinacolato) as a diborane. Furthermore, the addition of phosphine to the platinum catalyst reduced its activity. Rhodium phosphine complexes were proposed to be ineffective catalysts for the aldimine diboration. Wilkinson's catalyst [Rh(Cl)$(PPh_3)_3$] provides large amounts of the hydroboration product $ArCH_2$N(Bcat)R with respect to the diboration product.[37,43] It was proposed that the reason for the unselective reactivity is the poor regiocontrol of the C=N insertion step into a metal–boron bond. In the case of aldimines the formation of M–C and B–N bonds leads to diboration, whereas the formation of M–N and B–C bonds can cause β-hydrogen elimination reactions providing hydroboranes, which can then undergo hydroboration reactions.[37]

Baker and Westcott also investigated the rhodium-catalyzed borylation of ketimines with diboranes.[44] The use of acetophenone-derived imines PhC(CH_2R)=N(Ar) and $B_2cat'_2$ (cat′ = 4-^{t}Bu-1,2-O_2-C_6H_3) resulted in the formation of *N*-(boryl)enamines and *N*-borylamines. Combined DFT and ONIOM studies gave an insight into the mechanism.[45] An oxidative addition of the diborane at [Rh(Cl)$(PH_3)_3$] and imine coordination is followed by a regioselective insertion of the imine into the M–B bond by N–B bond formation. Then two possible steps can occur: either carbon–boron bond formation yields the desired diboration product or β-hydrogen elimination takes place to give the *N*-(boryl)enamines and HBcat′, which subsequently can add to the unreacted imine.

Humboldt-Universität zu Berlin, Department of Chemistry, Brook-Taylor-Straße 2, D-12489 Berlin, Germany. E-mail: thomas.braun@chemie.hu-berlin.de

†CCDC 977662–977667. For crystallographic data in CIF or other electronic format see DOI: 10.1039/c4dt00080c

Concerning the diboration of C=O double bonds, Sadighi *et al.* succeeded in the catalytic diboration of aldehydes using a unique copper(I) boryl complex, [(IPr)Cu(Bpin)] (IPr = 1,3-bis-(2,6-diisopropylphenyl)imidazol-2-ylidene), as a catalyst to give RCH(OBpin)Bpin.[46] A stoichiometric reaction of the complex with mesitylaldehyde generates [(IPr)Cu{CH(Ar)(OBpin)}], by the insertion of the carbonyl group into a metal–boron bond, which accompanied by a metal–carbon σ-bond formation. No evidence for the formation of the alternative regioisomer was found and an attempt to synthesize it using the appropriate alcohol failed giving the same product as for the insertion reaction of the aldehyde.[11] The catalytic diboration also proceeds using [(IPr)Cu{CH(Ar)(OBpin)}] as a catalyst or [(ICy)Cu-(O^{t}Bu)] (ICy = 1,3-cyclohexylimidazol-2-ylidene) as a precatalyst. The activity of these {(IPr)Cu} complexes in the catalytic diboration of ketones has also been demonstrated.[47–49]

Recently the synthesis of the 16-electron rhodium boryl complex [Rh(Bpin)(PEt$_3$)$_3$] (**1**)[50] was reported. This complex is capable of both, stoichiometric C–H and catalytic C–F or N–H bond activation reactions.[50,51] In this contribution we report on the reactivity of **1** towards ketones, ketimines and aldimines. The synthesis of rhodium complexes by insertion of C=O and C=N bond containing compounds into the Rh–B bond is described. Reactivity studies of these complexes bearing a Rh–C–O–B or a Rh–C–N–B linkage are also presented.

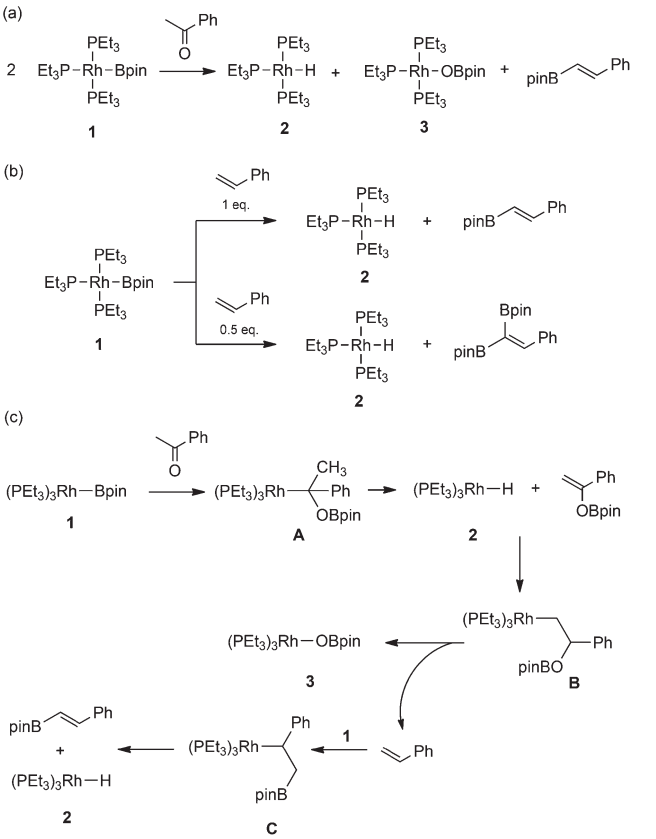

Scheme 1 Reactivity of complex **1** towards acetophenone (a) and styrene (b) and the proposed mechanism for the formation of (*E*)-(Ph)-CH=CHBpin (c).

Results and discussion

Reactivity of complex 1 towards ketones

Adding 0.5 equivalent of acetophenone to the boryl complex [Rh(Bpin)(PEt$_3$)$_3$] (**1**) resulted in the formation of [Rh(H)-(PEt$_3$)$_3$] (**2**) and [Rh(OBpin)(PEt$_3$)$_3$] (**3**) (Scheme 1a). Complex **3** was synthesized before and identified by comparison of the NMR data with an authentic sample. Moreover, the vinylboronate ester (*E*)-(Ph)CH=CHBpin was identified by ^{1}H and ^{13}C NMR spectroscopy. In addition traces of PhCH=C(Bpin)$_2$ could be detected by GC-MS analysis. The alkene PhC-(OBpin)=CH$_2$, which would be the result of a β-hydrogen elimination after insertion of the ketone into the Rh–B bond and O–B formation in **1**,[44] was not found.

Mechanistically we assume an initial insertion of the acetophenone into the Rh–B bond to produce complex **A**, which bears an oxygen–boron linkage (Scheme 1c). A β-hydrogen elimination step leads then to the formation of the hydrido complex **2** and PhC(OBpin)=CH$_2$. The latter might reinsert into the Rh–H bond to form complex **B**. Then, a migration of the borate ester entity to the metal results in the formation of **3** and the release of styrene. This alkene might react with additional boryl complex **1** by dehydrogenative borylation to give (*E*)-(Ph)CH=CHBpin[52–54] and **2**. Independent reactions support these suggestions. Treatment of **1** with stoichiometric amounts of styrene led selectively to **2** and (*E*)-(Ph)CH=CHBpin, as is depicted in Scheme 1b. Furthermore, a reaction of 0.5 equivalent alkene with **2** resulted in the formation of PhCH=C(Bpin)$_2$.

Apparently, the treatment of the boryl complex **1** with acetophenone leads to an insertion reaction, but the presence of a β-hydrogen atom at a ketone induces further reaction steps. To avoid the β-hydrogen elimination, we investigated the reactivity of the boryl complex **1** towards α,α,α-trifluoroacetophenone which bears fluorine instead of hydrogen atoms at the α-position. Adding α,α,α-trifluoroacetophenone to **1** gave instantaneously the rhodium η^3-benzyl complex [Rh{η^3-C(CF$_3$)-(OBpin)C$_6$H$_5$}(PEt$_3$)$_2$] (**4**) and one equivalent of phosphine, by insertion of the C=O double bond into the metal–boron bond (Scheme 2). Product **4** was characterized by NMR spectroscopy and liquid injection field desorption ionization mass spectrometry (LIFDI MS). LIFDI data revealed a peak at *m*/*z* 460 which can be assigned to the molecular ion [M]$^+$. The ^{31}P{^{1}H} NMR spectrum of **4** reveals two signals at δ 28.1 and 21.8 ppm due to the inequivalent phosphine ligands. The phosphorus–phosphorus coupling constant of 36 Hz is in the typical range for *cis*-phosphines.[55–57] The phosphorus–rhodium coupling constants of 257 Hz and 160 Hz are fairly large and indicate the presence of a rhodium(I) species.[55–57] The signal at δ 28.1 ppm with the larger phosphorus–rhodium coupling constant is caused by the phosphorus atom in the *trans* position to the ring according to extended Hückel MO calculations.[58,59]

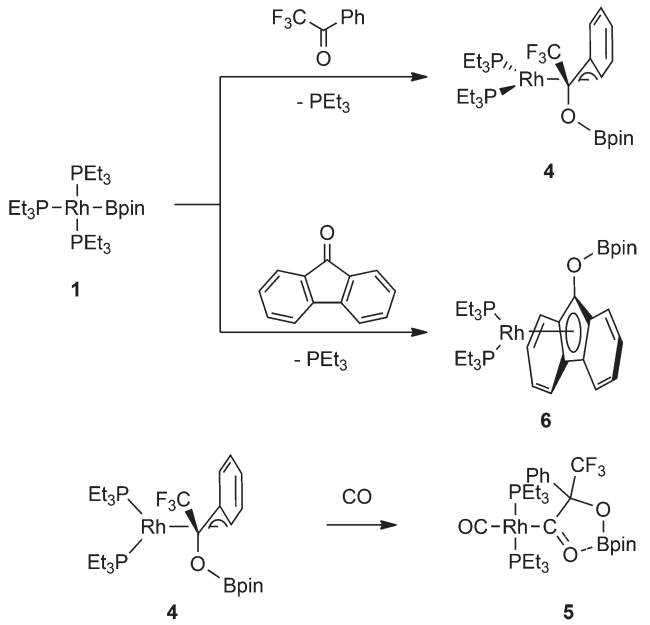

Scheme 2 Syntheses of complexes **4** and **6** and reactivity of complex **4** towards CO.

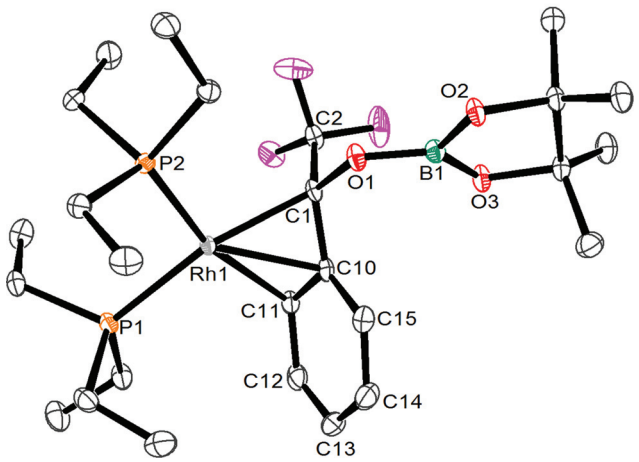

Fig. 1 An ORTEP diagram of **4**. The ellipsoids are drawn at the 50% probability level. The hydrogen atoms are omitted for clarity.

The signal at δ 21.8 ppm exhibits an additional coupling of 8 Hz to the fluorine atoms and can be assigned to the phosphine which is located in the *trans* position to the carbon atom bearing the CF_3 group. The presence of the latter moiety is also revealed in the ^{19}F NMR spectrum by a signal at δ −57.4 ppm. For the boron atom a resonance at δ 22.5 ppm can be detected in the ^{11}B NMR spectrum. The chemical shift is typical of a pinacol borate ester.[60–63] Complex **4** is not very stable in solution and decomposition starts within a few hours at room temperature according to the NMR spectra. In the presence of free phosphine its stability rises to one day.

The molecular structure of **4** was confirmed by single-crystal X-ray analysis (Fig. 1). Selected bond lengths and angles

Table 1 Selected bond lengths (Å) and angles (°) for **4** with estimated standard deviations in parentheses

Bond	Length	Bond	Angle
Rh1–C1	2.1248(14)	C1–Rh1–P2	99.37(4)
Rh1–C10	2.1929(14)	C1–Rh1–P1	164.60(4)
Rh1–C11	2.3833(15)	C10–Rh1–P1	127.20(4)
R1–P1	2.2850(4)	P2–Rh1–P1	95.936(14)
Rh1–P2	2.2274(4)	P2–Rh1–C11	166.06(4)
C1–O1	1.4244(17)	P1–Rh1–C11	97.61(4)
C1–C10	1.454(2)	O1–C1–C10	116.19(13)
C1–C2	1.504(2)	O1–C1–C2	107.33(12)
B1–O1	1.359(2)	C10–C1–C2	121.37(13)
C10–C11	1.422(2)	C10–C1–Rh1	72.86(8)
C10–C15	1.430(2)	C11–C10–C15	117.03(14)
C11–C12	1.415(2)	C11–C10–C1	120.51(14)
C12–C13	1.363(3)	C15–C10–C1	121.34(13)
C13–C14	1.408(3)	C10–C11–Rh	164.73(8)
C14–C15	1.368(2)		

are summarized in Table 1. The structure reveals an approximately square planar coordination geometry with P1, P2, C1 and C11 occupying the four coordination sites. The distance between the plane defined by these atoms and Rh1 is 0.04 Å. The dihedral angle between this plane and the plane defined by the benzyl group is 80.6° (for comparison 75.4° in [Rh(η^3-$CH_2C_6H_5$)(P*i*Pr$_3$)$_2$]).[59] The rhodium–carbon distances are 2.125(1) Å for Rh1–C1, 2.193(1) Å for Rh1–C10 and 2.383(2) Å for Rh1–C11 and are comparable to those found for [Rh(η^3-$CH_2C_6H_5$)(P*i*Pr$_3$)$_2$] (2.125(9), 2.23(1), 2.41(1) Å)[59] or [Rh(η^3-$CH_2C_6H_5$)(dippp)] (2.141(4), 2.197(3), 2.362(3) Å).[64] As a result of the coordination at the rhodium center the delocalization in the aromatic ring is repealed which is evidenced by short carbon–carbon distances for C12–C13 (1.363(3) Å) and C14–C15 (1.368(2) Å). The other ring carbon–carbon distances range between 1.408(3) and 1.430(2) Å.

Treatment of the rhodium(I) benzyl complex **4** with CO led to the insertion of CO into the rhodium–carbon bond as well as to CO coordination (Scheme 2). The generation of *trans*-[Rh{C(O)C(CF_3)(Ph)OBpin}(CO)(PEt$_3$)$_2$] (**5**) can be observed by a color change from dark red to yellow and the precipitation of a hardly soluble solid. The formation of **5** is in sharp contrast to a report by Werner *et al.*, who treated [Rh(η^3-$CH_2C_6H_5$)(P*i*Pr$_3$)$_2$] with CO, which gave [Rh(η^1-$CH_2C_6H_5$)(CO)(P*i*Pr$_3$)$_2$].[59] In **5** an intramolecular B–O interaction between the Lewis-acidic boron atom and the oxygen atom of the C=O unit seems to favor the CO insertion and leads to a five membered ring formation. The $^{31}P\{^1H\}$ NMR spectrum of **5** displays a doublet of doublets at δ 25.6 ppm and a doublet of doublet of quartets at δ 22.7 ppm. The resonances reveal a phosphorus–phosphorus coupling of 210 Hz for the phosphorus atoms, which are oriented in a mutual *trans* position. The phosphorus–rhodium coupling constants of both signals are 141 Hz and comparable to that in *trans*-[Rh(Me)(CO)(PEt$_3$)$_2$] (J_{RhP} = 140 Hz).[65] A quartet splitting is caused by a fluorine–phosphorus coupling of 4 Hz. The same coupling constant is found in the $^{19}F\{^1H\}$ NMR spectrum for a signal at δ −71.8 ppm. For the boron atom a resonance is detected at δ

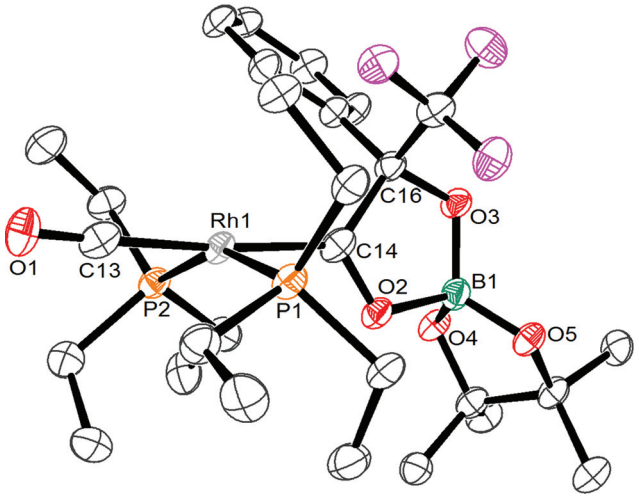

Fig. 2 An ORTEP diagram of **5**. The ellipsoids are drawn at the 50% probability level. The hydrogen atoms are omitted for clarity.

Table 2 Selected bond lengths (Å) and angles (°) in **5** with estimated standard deviations in parentheses

Bond	Length	Bond	Angle
Rh1–C13	1.878(4)	C13–Rh1–C14	175.04(15)
Rh1–C14	2.016(4)	C13–Rh1–P1	91.12(11)
Rh1–P1	2.3100(9)	C14–Rh1–P1	91.59(10)
Rh1–P2	2.3333(10)	C13–Rh1–P2	88.62(12
O1–C13	1.147(5)	C14–Rh1–P2	90.71(11)
O2–C14	1.266(4)	P1–Rh1–P2	154.61(4)
O2–B1	1.616(4)	C14–O2–B1	114.2(3)
O3–C16	1.401(4)	C16–O3–B1	114.3(3)
O3–B1	1.450(5)	O1–C13–Rh1	177.5(3)
O4–B1	1.427(5)	O2–C14–C16	107.1(3)
O5–B1	1.423(4)	O5–B1–O4	108.4(3)
C14–C16	1.580(5)	O5–B1–O3	118.2(3)
		O4–B1–O2	108.8(3)
		O3–B1–O2	98.7(3)
		O3–C16–C14	105.5(3)

15.3 ppm in the ^{11}B NMR spectrum. This resonance is shifted to higher field when compared to the signal of **4** or to other pinacol esters of boric acids, and to lower field when compared to the resonance for borate anions ($[B(pin)_2]^-$: δ 8 ppm).[66] The IR spectrum of **5** reveals absorption bands at 1952 cm^{-1} and 1478 cm^{-1} which are characteristic for a rhodium(I) carbonyl ligand and for the acyl moiety, respectively.[67,68] Note that the rhodium acyl complex [Rh{C(O)CH$_2$Ph}(CO)$_2$(κ^2-*i*Pr$_2$PCH$_2$-P*i*Pr$_2$)] exhibits an absorption band at 1714 cm^{-1} in the IR spectrum.[69] The isotopologue of **5**, *trans*-[Rh{^{13}C(O)C(CF$_3$)(Ph)-OBpin}(^{13}CO)(PEt$_3$)$_2$] (**5a**), was obtained on treatment of **4** with ^{13}CO. The ^{13}C NMR spectrum shows one doublet of doublet of triplets at δ 198.7 ppm which can be assigned to the carbonyl ligand and one at δ 296.1 ppm indicating the presence of the acyl moiety. The carbon–rhodium and the carbon–phosphorus coupling constants have characteristic values of 52 Hz (C≡O), 42 Hz (C=O) and 16 Hz (C≡O), 12 Hz (C=O).[67] The carbon–carbon coupling is 34 Hz. The signals of **5a** in the ^{31}P{^{1}H} NMR spectrum exhibit two additional carbon–phosphorus couplings in comparison to **5**.

The molecular structure of **5** was confirmed by single-crystal X-ray analysis (Fig. 2). Selected bond lengths and angles are summarized in Table 2. The rhodium atom is coordinated by a CO ligand, an acyl unit and two phosphine ligands. The square-planar geometry is strongly distorted as evidenced by a P1–Rh1–P2 angle of 154.61(4)° and a C13–Rh1–C14 angle of 175.04(15)°. The metal–carbon bond length to the carbonyl ligand of 1.878(4) Å is comparable to that in *trans*-[Rh(4-C$_5$NF$_4$)-(CO)(PEt$_3$)$_2$] (1.8494(16) Å).[67] The rhodium–carbon distance Rh1–C14 of 2.016(4) Å is relatively short, but comparable with the bond in other rhodium(III) acyl complexes like [RhI(COMe)-(4-C$_5$NF$_4$)(PEt$_3$)$_2$] (2.0018(19) Å).[67,70] The short distance between the boron atom and the oxygen atom in the acyl moiety of 1.616(4) Å (for comparison the B–O bond lengths in the borate ester moiety are 1.423(4) to 1.450(5) Å) and the nearly tetrahedral geometry at the boron atom indicate an interaction between the Lewis-acid boronic ester and the carbonyl group. A similar result was found for *N*-(2-(4,4,5,5-tetramethyl-1,3,2-dioxaboronlan-2-yl)phenyl)acetamide, where an interaction between the boron atom and the oxygen atom of the acetamide group leads to a B–O distance of 1.598(3) Å.[71] This interaction effects the ring formation and an elongation of the C14–O2 bond to be 1.266(4) Å. The comparable distance in [Rh(I)(COMe)(4-C$_5$NF$_4$)(PEt$_3$)$_2$] is 1.202(2) Å.[67]

Treatment of the rhodium(I) boryl complex **1** with 9-fluorenone yielded the C=O insertion product [Rh{η^5-C$_{13}$H$_8$(OBpin)}-(PEt$_3$)$_2$] (**6**) as well as free phosphine within one hour (Scheme 2). The formally negative charge at the metal bound fluorene is likely to be delocalized in the five-membered ring, which is consistent with an η^5-coordination of the fluorenyl ligand at the rhodium atom in **6**. Complex **6** was characterized by NMR spectroscopy and elemental analysis. The ^{31}P{^{1}H} NMR spectrum of **6** displays two doublet of doublets at δ 40.7 and 19.8 ppm. The phosphorus–rhodium coupling constants are 254 Hz and 204 Hz and the phosphorus–phosphorus coupling constant is 43 Hz. This pattern confirms again the presence of a rhodium(I) species with a *cis* alignment of the two phosphine ligands. The presence of the borate ester moiety is revealed in the ^{11}B NMR spectrum by a signal at δ 22.7 ppm. The ^{1}H and ^{13}C NMR spectra of **6** exhibit signals in the aromatic region caused by the fluorenyl group. Compound **6** exhibits a pronounced sensitivity towards air and moisture as solid as well as in solution. The solubility in hexamethyldisilane, hexane or benzene is very low.

The identity of **6** was further confirmed by single-crystal X-ray analysis. An ORTEP drawing is presented in Fig. 3, whereas selected bond distances and angles are reported in Table 3. The rhodium atom is coordinated by two phosphorus atoms with a P1–Rh–P2 angle of 97.51(3)° and one fluorenyl ligand with a rhodium–centroid distance of 1.9847(12) Å. The P1–Rh–P2 plane is nearly perpendicular to the plane defined by the fluorenyl system (dihedral angle: 88.54(12)°). There are five short (Rh1–C1 2.217(3) Å, Rh1–C2 2.355(3) Å, Rh1–C5 2.355(3) Å, Rh1–C3 2.360(3) Å, Rh1–C4 2.365(3) Å) rhodium–

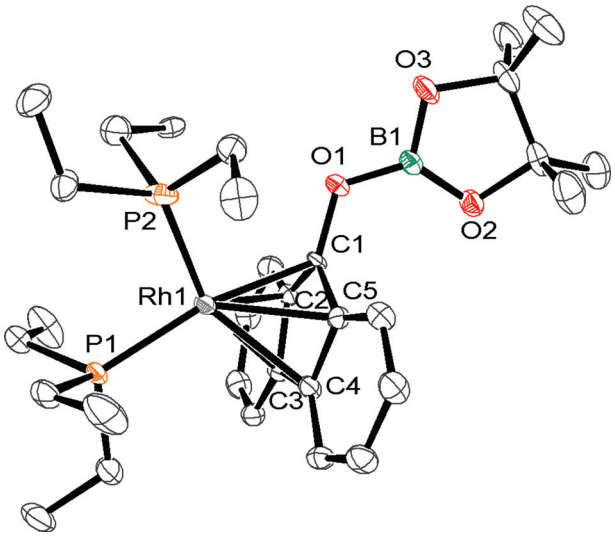

Fig. 3 An ORTEP diagram of **6**. The ellipsoids are drawn at the 50% probability level. The hydrogen atoms are omitted for clarity.

Table 3 Selected bond lengths (Å) and angles (°) for **6** with estimated standard deviations in parentheses

Bond	Length	Bond	Angle
Rh1–P1	2.2573(8)	P2–Rh1–C1	96.30(8)
Rh1–P2	2.2040(9)	P2–Rh1–P1	97.51(3)
Rh1–C1	2.217(3)	C1–Rh1–P1	165.35(8)
Rh1–C2	2.355(3)	P1–Rh1–C2	130.67(9)
Rh1–C5	2.355(3)	P1–Rh1–C5	139.29(8)
Rh1–C3	2.360(3)	P1–Rh1–C3	104.94(8)
Rh1–C4	2.365(3)	P1–Rh1–C4	109.23(8)
O1–B1	1.371(4)	B1–O1–C1	122.4(3)
O1–C1	1.392(4)	O1–C1–C5	125.5(3)
C1–C5	1.432(4)	O1–C1–C2	123.5(3)
C1–C2	1.433(4)	C5–C1–C2	109.5(3)
C2–C3	1.433(4)	C3–C2–C1	107.2(3)
C3–C4	1.467(4)	C2–C3–C4	107.3(3)
C4–C5	1.429(5)	C5–C4–C3	108.2(3)
		C4–C5–C1	106.9(3)

carbon bond lengths, indicating a η^5 coordination. The geometry at the carbon atom C1 is nearly trigonal-planar with an angular sum of 358.5(3)°.

Reactivity of complex 1 towards imines

The boryl complex [Rh(Bpin)(PEt_3)$_3$] (**1**) also reacted with the ketimines, *N*-(diphenylmethylene)aniline or *N*-(fluoren-9-ylidene)aniline (Scheme 3). Adding the latter compounds to a solution of **1** in Me_6Si_2 resulted in the formation of a red or purple solid within one day or half an hour, respectively. In a comparable way to the insertion reactions of ketones, the complexes [Rh{η^3-C_6H_5=C(Ph)N(Ph)(Bpin)}(PEt_3)$_2$] (**7**) and [Rh{(η^3-$C_{12}H_8$)N(Ph)(Bpin)}(PEt_3)$_2$] (**8**) were furnished by insertion of the C–N double bond into the rhodium–boron bond, and N–B bonds are generated. However, in each case the rhodium atom is coordinated in a remote position at an aromatic ring, which results in an enamine structure.

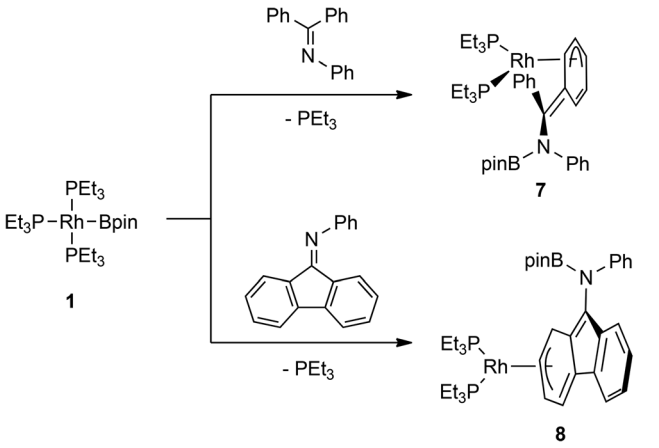

Scheme 3 Syntheses of complexes **7** and **8**.

Complexes **7** and **8** could be isolated and were characterized by NMR spectroscopy. The $^{31}P\{^1H\}$ NMR spectrum at 293 K of **7** reveals two broad doublets at δ 31.8 and 30.5 ppm in a 5 : 1 ratio, which can be assigned to two isomeric structures. The phosphorus–rhodium coupling constant for each signal is 212 Hz, indicating the presence of rhodium(I) complexes. NMR analysis of a solution of **7** at higher temperature shows that the two resonances are coalesced at 333 K and the rhodium–phosphorus coupling constant is retained (Fig. 4). For compound **8**, a single resonance at δ 34.2 ppm can be detected in the $^{31}P\{^1H\}$ NMR spectrum, which exhibits a phosphorus–rhodium coupling constant of 215 Hz. Variable-temperature NMR analysis of a solution of **8** shows that the resonance splits into two signals at low temperature. The ratio of the signals is temperature-dependent (1 : 0.55 at 243 K), which also suggests an equilibration between two isomers. We assume that the presence of two isomers of **7** and **8** is caused by a restricted rotation about the C–N bond. In addition the variable-temperature $^{31}P\{^1H\}$ NMR analysis of a solution of **7** indicates a dynamic behavior, which presumably involves an additional intramolecular exchange of the phosphine ligands in the isomers. Thus, the NMR spectrum at 253 K exhibits a very broad signal for the major isomer, which splits into two signals at 223 K. At 203 K the expected pattern of a doublet of doublets at δ 35.5 ppm and a doublet of doublets at δ 29.5 ppm with coupling constants of 210 and 213 Hz (J_{RhP}) as well as of 46 Hz (J_{PP}) was observed. At 223 K the signal for the minor isomer starts to decoalesce (Fig. 4). For the boron atoms in complexes **7** and **8** resonances can be detected in the ^{11}B NMR spectrum at δ 25.2 (**7**) and 24.8 ppm (**8**), respectively. They appear in the typical range for aminoborate esters.[51,72,73]

The molecular structures of **7** and **8** were confirmed by single-crystal X-ray analysis (Fig. 5 and 6). Selected bond lengths and angles are summarized in Tables 4 and 5. The asymmetric unit of **7** includes two crystallographically independent molecules, which show only minor differences in the bond length and angles. Therefore, only one of the two crystallographically independent molecules is shown and discussed. In the structure of **7** the central rhodium atom is coordinated by two

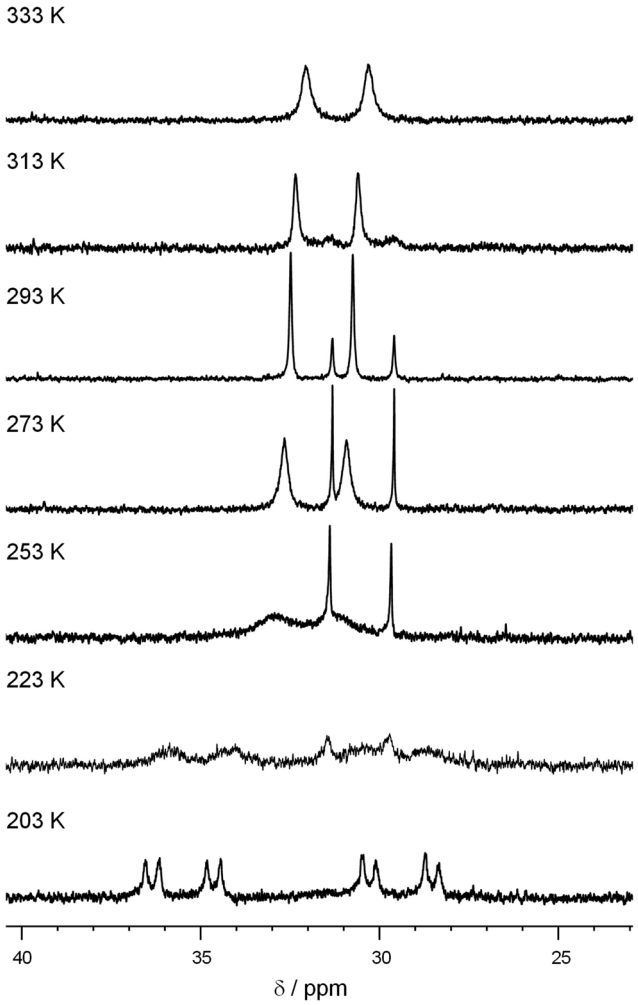

Fig. 4 Variable temperature $^{31}P\{^{1}H\}$ NMR spectra (121.5 MHz, $[D_8]$toluene) of **7**.

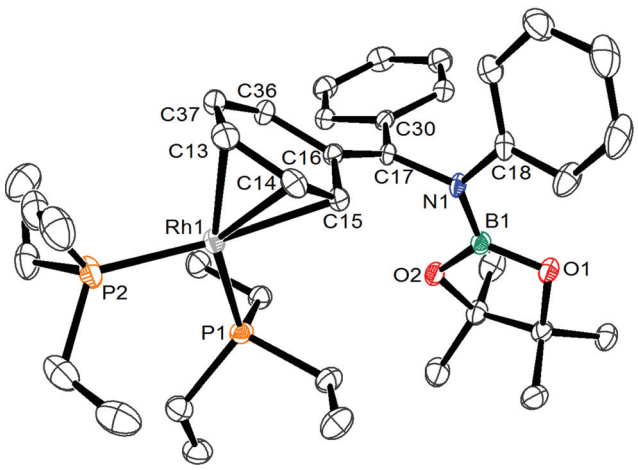

Fig. 5 An ORTEP diagram of **7**. The ellipsoids are drawn at the 50% probability level. The hydrogen atoms are omitted for clarity. The asymmetric unit cell contains two crystallographically independent molecules; only one of them is shown.

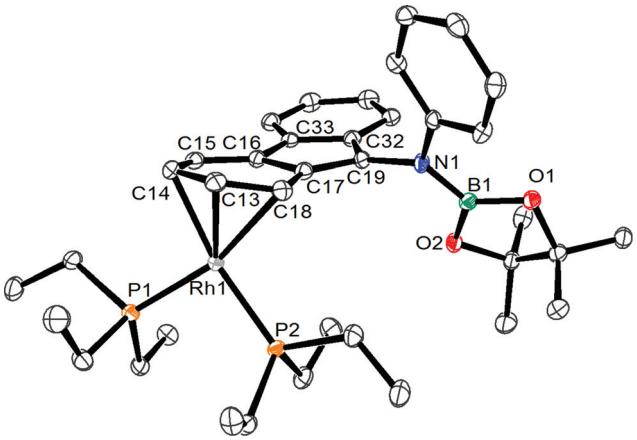

Fig. 6 An ORTEP diagram of **8**. The ellipsoids are drawn at the 50% probability level. The hydrogen atoms are omitted for clarity.

Table 4 Selected bond lengths (Å) and angles (°) for **7** with estimated standard deviations in parentheses (the data for the second crystallographically independent molecules are comparable and are therefore not shown)

Bond	Length	Bond	Angle
Rh1–C13	2.201(2)	C13–Rh1–P2	99.44(7)
Rh1–C14	2.212(2)	C13–Rh1–P1	161.64(7)
Rh1–P2	2.2299(6)	P2–Rh1–P1	98.87(2)
Rh1–P1	2.2477(6)	P2–Rh1–C15	159.83(6)
Rh1–C15	2.312(2)	P1–Rh1–C15	97.12(6)
Rh1–C16	2.793(2)	C18–N1–B1	124.70(17)
Rh1–C36	2.695(2)	C18–N1–C17	116.60(17)
Rh1–C37	2.437(2)	B1–N1–C17	117.74(18)
N1–C18	1.424(3)	C14–C13–C37	118.2(2)
N1–B1	1.423(3)	C15–C14–C13	118.6(2)
N1–C17	1.452(2)	C14–C15–C16	123.07(19)
C13–C14	1.411(3)	C17–C16–C36	125.3(2)
C13–C37	1.432(4)	C17–C16–C15	121.61(18)
C14–C15	1.401(3)	C36–C16–C15	113.1(2)
C15–C16	1.463(3)	C16–C17–N1	118.11(19)
C16–C17	1.370(3)	C37–C36–C16	121.1(2)
C16–C36	1.461(3)	C36–C37–C13	122.8(2)
C36–C37	1.373(3)		

phosphine ligands with a P1–Rh–P2 angle of 99.44(7)° and an allylic moiety. Three short rhodium–carbon bond lengths (Rh1–C13 2.201(2) Å, Rh1–C14 2.212(2) Å, Rh1–C15 2.312(2) Å) indicate η^3 coordination. The distance between the rhodium atom and the plane defined by the carbon atoms C13, C14, C15, C16, C36 and C37 is 1.92836(17) Å. This plane is perpendicular to the P1–Rh1–P2 plane with a dihedral angle of 89.14(9)°. The Bpin group is arranged on the same side as the metal atom with regard to the PhCN moiety. The geometry at the carbon atom C17 is nearly trigonal-planar which is indicated by an angular sum of 359.72(10)°. The C16–C17 bond distance of 1.370(3) Å is significantly shorter than the C17–C30 bond length (1.464(3) Å) and can be assigned to a carbon–carbon double bond[74] which verifies the formation of an enamine. The carbon–carbon bond distance C36–C37 (1.373(3) Å) is also very short, whereas the other C–C bond lengths in the

Table 5 Selected bond lengths (Å) and angles (°) for **8** with estimated standard deviations in parentheses

Bond	Length	Bond	Angle
Rh1–C14	2.206(3)	C14–Rh1–P1	98.55(8)
Rh1–P1	2.2245(7)	C14–Rh1–P2	162.27(7)
Rh1–C13	2.235(3)	P1–Rh1–P2	95.03(3)
Rh1–P2	2.2377(8)	P1–Rh1–C18	159.72(7)
Rh1–C18	2.347(3)	P2–Rh1–C18	99.46(7)
Rh1–C15	2.409(3)	B1–N1–C19	118.9(2)
Rh1–C16	2.682(3)	C18–C13–C14	119.5(2)
Rh1–C17	2.706(3)	C13–C14–C15	119.7(3)
N1–B1	1.421(4)	C16–C15–C14	120.8(2)
N1–C19	1.437(3)	C15–C16–C17	120.1(2)
C13–C18	1.408(4)	C19–C17–C18	132.8(2)
C13–C14	1.417(4)	C19–C17–C16	109.6(2)
C14–C15	1.431(4)	C18–C17–C16	117.6(2)
C15–C16	1.385(4)	C13–C18–C17	120.4(2)
C16–C17	1.459(4)	C16–C17–C19	109.6(2)
C16–C33	1.452(4)	C19–C32–C33	109.3(2)
C17–C19	1.386(4)		
C17–C18	1.439(4)		
C19–C32	1.433(4)		
C32–C33	1.429(4)		

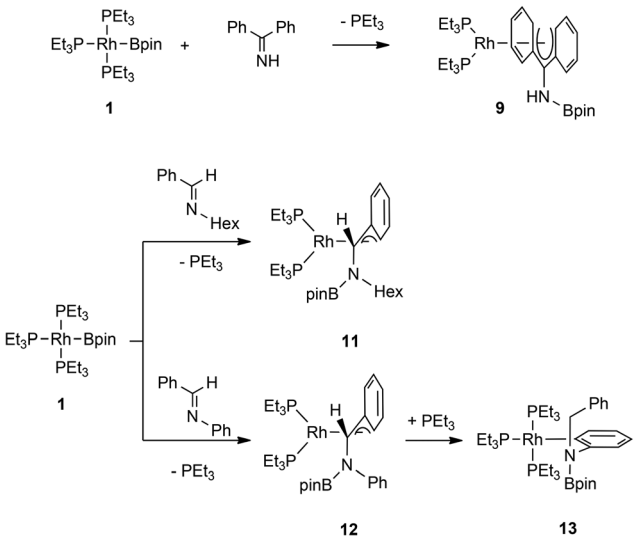

Scheme 4 Syntheses of complexes **9**, **9′** and **11–13**.

metal bound ring are in the range of 1.401(3) to 1.463(3) Å (for the η^3-allyl entity: 1.401(3) and 1.411(3) Å). The C17–N1 bond length (1.452(2) Å) is long for a C═C–NR_2 bond,[75] which is probably caused in part by the presence of the boryl moiety with the empty orbital at the boron atom. However it is comparable with the corresponding bond lengths of 1.424(3) Å in **7**, 1.437(3) Å in **8** as well as 1.442(3) Å and 1.458(3) Å in **13**. The bonding situation in **8** is comparable to the one in **7**. The rhodium atom is coordinated by two phosphines with a P1–Rh–P2 angle of 98.55(8)° and in a η^3-fashion by the fluorenyl ligand. The distance of the plane defined by the carbon atoms C13, C14, C15, C16, C17 and C18 to the metal atom is 1.9264(2) Å and in a similar range as it was found for complex **7**. Again, this plane is nearly perpendicular to the P1–Rh–P2 plane (dihedral angle: 84.25(9)°) and the aminoborate ester moiety is arranged on the same side as the rhodium atom with respect to the plane defined by the fluorenyl ligand. The crystal data reveal three short (Rh1–C14 2.206(3) Å, Rh1–C13 2.235(3) Å, Rh1–C18 2.347(3) Å) and one medium (Rh1–C15 2.409(3) Å) rhodium–carbon bond lengths. The geometry at the carbon atom C19 is nearly trigonal-planar with an angular sum of 359.7(2)°. A distance of the C17–C19 bond of 1.386(4) Å confirms the presence of a double bond.

In addition, we investigated the reactivity of the boryl complex **1** towards a ketimine which does not carry any further substituent at the nitrogen atom. Adding benzophenone imine to a solution of **1** led to the insertion of the imine into the rhodium–boron bond. A complete conversion was observed within seconds to give the complex [Rh{CPh_2N(H)(Bpin)}-(PEt_3)$_2$] (**9**, Scheme 4) and free phosphine. Note that the formation of [Rh{N═CPh_2}(PEt_3)$_3$] (**10**)[76] and HBpin was observed when the reaction solution was highly concentrated or when the organic substrate was added rapidly to **1**.

Without the presence of free phosphine complex **9** decomposes very fast, and even in the presence of free phosphine complex **9** is only stable for a few hours at room temperature. Therefore complex **9** was identified by NMR spectroscopy and LIFDI MS only. The latter reveals a peak at *m*/*z* 647 which can be assigned to the molecular ion $[M]^+$. The $^{31}P\{^1H\}$ NMR spectrum of **9** at room temperature shows two doublet of doublets at δ 22.3 and 18.7 ppm with phosphorus–rhodium coupling constants of 163 Hz and 262 Hz as well as a phosphorus–phosphorus coupling constant of 32 Hz. The coupling constants are in accordance with the presence of a Rh(I) complex and comparable to those found for **4**, **11** and **12** (see below). Complex **9** exhibits a signal at δ 24.6 ppm in the ^{11}B NMR spectrum which indicates the presence of the aminoborate ester moiety. The ^1H NMR spectrum of **9** displays only three resonances in the aromatic region in a ratio of 4 : 4 : 2, and the ^{13}C NMR spectrum shows three resonances for CH carbon atoms in the aromatic region. This suggests the presence of a complex which is fluxional on the NMR time scale rendering some of the CH units to be equivalent. The formation of an intermediate η^3-benzyl complex might result in equivalent hydrogen and carbon atoms by a rotation of the phenyl groups.

Variable temperature $^{31}P\{^1H\}$ NMR spectra of a solution of **9** and free phosphine show at low temperature (<273 K) the presence of **9** and of a second complex **9′** for which we suggest the structure to be [Rh{η^1-CPh_2N(H)(Bpin)}(PEt_3)$_3$] (Fig. 7). The broadness of the signals of **9′** and of PEt_3 might possibly be attributed to an intermolecular exchange with free phosphine. The exchange would have to be associative, because the resonances for **9** remain sharp at 273 K, implying that **9′** does not get converted into **9**. However, we were not able to identify a signal for **9′** at higher temperatures, because of a rapid decomposition. However, at 253 K the signal for PEt_3 sharpens whereas a broad doublet at δ 13.8 ppm with a phosphorus–rhodium coupling constants of 145 Hz for **9′** can be observed. The broadening indicates an intramolecular exchange process

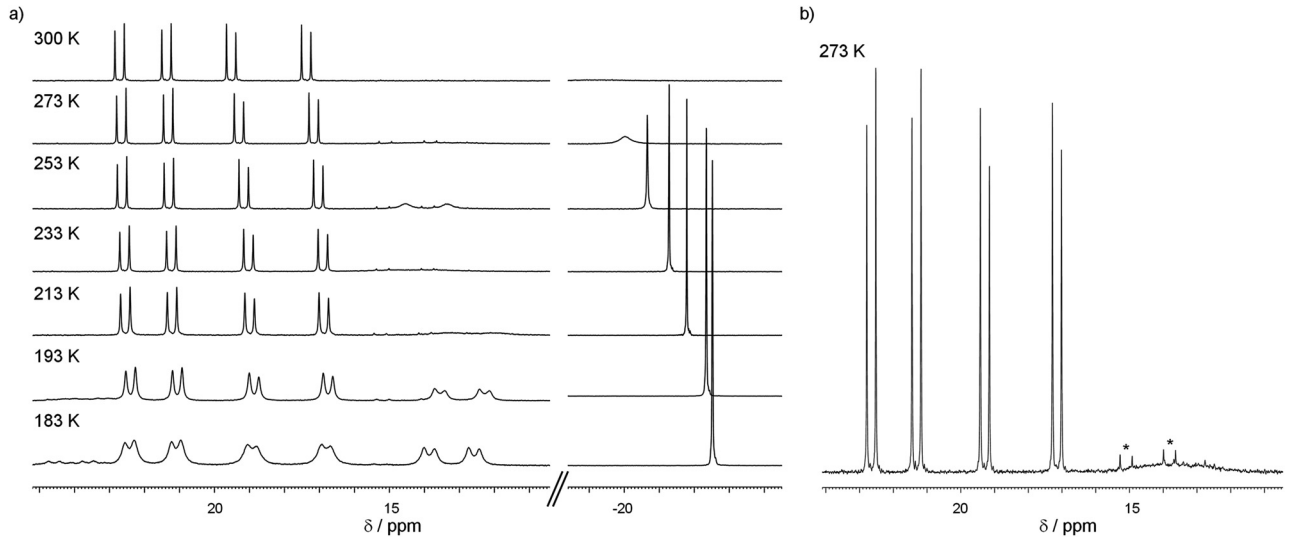

Fig. 7 (a) Variable temperature $^{31}P\{^1H\}$ NMR spectra (121.5 MHz, $[D_8]$toluene) of a solution of **9** and **9′**. (b) Magnification of the $^{31}P\{^1H\}$ NMR spectrum (121.5 MHz, $[D_8]$toluene) at 273 K (*: traces of **10**).

of the phosphine ligands at **9′**. Further decrease of the temperature to 188 K leads to a splitting into two signals at δ 23.7 and 13.1 ppm in a ratio of 1 : 2, which suggests the presence of a square planar rhodium complex bearing three PEt_3 ligands. The phosphorus–rhodium coupling constants of 119 Hz and 155 Hz indicate the presence of a Rh(I) species and the phosphorus–phosphorus coupling constant of 37 Hz is in a typical range for phosphine ligands in a mutual *cis*-position.[50,51,55–57,77] We suggest **9′** to be the σ-complex $[Rh\{\eta^1\text{-}CPh_2N(H)(Bpin)\}(PEt_3)_3]$ with the anionic ligand bound to rhodium *via* the CPh_2 carbon atom due to the similarity of the $^{31}P\{^1H\}$ NMR data for organorhodium(I) complexes $[Rh(R)(PEt_3)_3]$.[56,76] The presence of three phosphine ligands argues against an η^3-benzylic structure.[55,59,78,79]

Whereas benzaldehyde does not react with **1** in a selective way, a selective insertion reaction at **1** with aldimines was observed. Treatment with *N*-benzylidenehexan-1-amine generated free phosphine and complex **11**, for which we suggest a benzylic structure $[Rh[\eta^3\text{-}CH\{N(C_6H_{13})Bpin\}C_6H_5](PEt_3)_2]$ (**11**) (Scheme 4). Complex **11** was characterized by NMR spectroscopy and LIFDI MS. The LIFDI data reveal a peak at *m*/*z* 460 which can be assigned to the molecular ion $[M]^+$. The $^{31}P\{^1H\}$ NMR spectrum of **11** exhibits two doublets of doublets at δ 25.8 and 21.7 ppm. The phosphorus–rhodium coupling constant of 270 Hz or 168 Hz is comparable to those which were determined for **4** and **9** and again confirm the oxidation state of Rh(I).[55–57] The phosphorus–phosphorus coupling constant of 26 Hz is relatively small. Analogous to **4** the ^1H NMR spectrum displays three broad signals in the aromatic region. Furthermore, a signal at δ 4.15 ppm with a phosphorus–hydrogen coupling of 5 Hz can be assigned to the benzylic proton. These NMR spectroscopic data indicate the presence of an η^3-benzyl complex.

Initially, the reaction of **1** with *N*-benzylideneaniline proceeded in a similar way and the benzyl complex $[Rh[\eta^3\text{-}CH\{N(Ph)Bpin\}C_6H_5](PEt_3)_2]$ (**12**) was obtained. But within 10 minutes the reaction solution changed its color and NMR spectroscopic studies revealed the formation of $[Rh\{(C_6H_4)\text{-}o\text{-}N(Bpin)(CH_2Ph)\}(PEt_3)_3]$ (**13**) and the decrease of the amount of **12** and of free phosphine (Scheme 4). Complex **13** is generated by C–H activation at the N-bound phenyl ring and a concomitant C–H bond formation at the benzyl moiety. Complex **12** was only characterized in solution by ^1H and $^{31}P\{^1H\}$ NMR spectroscopy. The spectra resemble those of **11**. The $^{31}P\{^1H\}$ NMR spectrum of **13** shows two signals in a ratio of 1 : 2. The chemical shift and the phosphorus–rhodium and phosphorus–phosphorus coupling constants are in agreement with those found for other aryl complexes.[80] A resonance at δ 24.8 ppm in the ^{11}B NMR spectrum indicates the presence of the N–Bpin bond.

The molecular structure in the solid-state of **13** was determined by single-crystal X-ray diffraction. An ORTEP drawing is presented in Fig. 8, whereas selected bond distances and angles are reported in Table 6. The rhodium atom is coordinated by the aryl ligand and three phosphine ligands in an approximately square planar geometry. The aryl plane is arranged in an orthogonal position to the plane defined by the atoms P1, P2, P3, C19 and Rh1 (dihedral angle: 82.96(15)°). The Rh–C19 distance of 2.077(3) Å and the Rh–P distances agree well with the corresponding distances found for $[Rh(C_6H_4\text{-}o\text{-}OMe)(PEt_3)_3]$.[56]

Consecutive reactions

With regard to a diboration reaction we also investigated the reactivity of the insertion reaction products towards B_2pin_2.

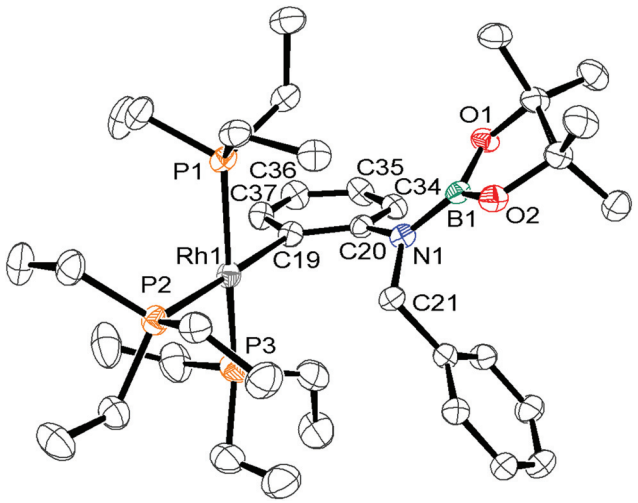

Fig. 8 An ORTEP diagram of **13**. The ellipsoids are drawn at the 50% probability level. The hydrogen atoms are omitted for clarity.

Table 6 Selected bond lengths (Å) and angles (°) for **13** with estimated standard deviations in parentheses

Bond	Length	Bond	Angle
Rh1–C19	2.077(3)	C19–Rh1–P1	83.60(7)
Rh1–P1	2.3094(7)	C19–Rh1–P2	177.39(8)
Rh1–P2	2.3245(8)	P1–Rh1–P2	94.23(3)
Rh1–P3	2.3364(8)	C19–Rh1–P3	81.78(8)
N1–B1	1.404(4)	P1–Rh1–P3	161.99(3)
N1–C20	1.442(3)	P2–Rh1–P3	100.61(3)
N1–C21	1.458(3)	B1–N1–C20	124.1(2)
C19–C37	1.413(4)	B1–N1–C21	115.7(2)
C19–C20	1.422(4)	C20–N1–C21	120.1(2)
C20–C34	1.400(4)	C37–C19–C20	115.2(3)
C34–C35	1.386(4)	C37–C19–Rh1	118.7(2)
C35–C36	1.381(4)	C20–C19–Rh1	126.1(2)
C36–C37	1.385(4)	C34–C20–C19	121.0(2)

Unfortunately, in most of the cases either no reaction occurred or only reaction mixtures were generated, for which none of the products could be identified apart from complex **1**. However, complex **9** reacted at room temperature with B_2pin_2 in the presence of phosphine in cyclohexane within a few hours to yield **1** (Scheme 5). The formation of **1** was confirmed by $^{31}P\{^1H\}$ NMR spectroscopy. The ^1H NMR and ^{13}C NMR spectra revealed the generation of $Ph_2CHN(H)Bpin$ as the only organic product. Only minor amounts of the diboration product $Ph_2C(Bpin)N(H)Bpin$ were formed according to GC-MS analysis. In principle $Ph_2CHN(H)Bpin$ could be generated by hydrolysis, but the presence of adventitious water is not very likely, because in the presence of water **1** would be converted into $[Rh(H)(PEt_3)_3]$ (**2**). In addition, the N–Bpin bond is labile and aminoborate esters like $Ph_2CHN(H)Bpin$ have a high reactivity towards water or even alcohols.[73,81] At present, the source of the NH hydrogen atom in $Ph_2CHN(H)Bpin$ is unclear. Note that the $[Rh(Cl)(PPh_3)_3]$ catalyzed reaction of aldimines with diboranes also led to hydroboration products amongst others.[37,43] Comparable observations have been reported with Pt and Cu catalysts.[81–84] However, in the latter cases water or protic solvent was used for the reaction work-up.

Treatment of **4** with B_2pin_2 also did not lead to any diboration. Instead the generation of the boryl complex **1** and of $PhCH(OBpin)CF_3$ was observed. In addition, $[Rh\{C(=CF_2)Ph\}(PEt_3)_3]$ (**14**), FBpin as well as pinBOBpin were identified (Scheme 5). The $^{31}P\{^1H\}$ NMR spectrum of **14** displays a resonance for the phosphine in the *trans* position to the vinyl ligand at δ 20.1 ppm. It appears as a doublet of triplet of doublet of doublets due to couplings to the rhodium, phosphorus and the fluorine atoms. The coupling pattern of the resonance at δ 11.6 ppm, which can be assigned to the phosphine ligands in a mutual *cis* position, appears as a doublet of doublet of doublets and exhibits couplings to rhodium, phosphorus and one of the fluorine atoms. The ^{19}F NMR spectrum shows signals at δ −75.1 and −69.3 ppm. The formation of **14** can tentatively be explained by initial generation of the carbene complex $[Rh(Bpin)_2(OBpin)(=CPhCF_3)(PEt_3)_2]$ from **4** by oxidative addition of B_2pin_2 and OBpin migration to the metal center. Elimination of pinBOBpin might yield the rhodium boryl complex $[Rh(Bpin)(=CPhCF_3)(PEt_3)_2]$.[50,51] A subsequent β-F-elimination step and FBpin formation by reductive elimination gives the fluorovinyl ligand and complex **14**.[85–87] As an alternative, the fluorine atom can be transferred directly to the metal-bound boryl moiety. There are some precedents for boryl-assisted and other comparable ligand-assisted C–F activation reactions in the literature.[22,50,85,88–95]

The aryl complex **13** successfully reacted with B_2pin_2 within 16 h at 50 °C to yield the boryl complex **1** and the diborylated amine $PhCH_2N(Bpin)(C_6H_4$-*o*-$Bpin)$ (Scheme 5). The latter was characterized by NMR spectroscopy and GC-MS analysis. In the ^{11}B NMR spectrum a resonance at δ 28.9 ppm for the boronate ester moiety and a resonance at δ 24.6 ppm for the aminoborate ester group were detected. Catalytic investigations by treatment of *N*-benzylideneaniline with B_2pin_2 in the presence of **1** led to a product mixture.

Conclusions

We have reported on the reactivity of a rhodium boryl complex towards carbon–heteroatom double bonds. Complex $[Rh(Bpin)(PEt_3)_3]$ (**1**) reacts with ketones, aldimines and ketimines by insertion of the C=O or the C=N entities into the Rh–B bond to give a boron–oxygen or a boron–nitrogen bond. In the presence of an aromatic system, stabilization of the products occurs by η^3 or η^5 coordination, and a variety of bonding modes was observed. The presence of β-hydrogen atoms can lead to β-H-elimination. Although the insertion of carbon–heteroatom double bonds into metal–boron bonds was suggested before in metal-catalyzed hydroboration and diboration reactions, this important key step was never observed in a model reaction. The insertion products of ketones are the first examples of such a type of compounds and their formation supports the proposed mechanisms.[47] Moreover, the insertion

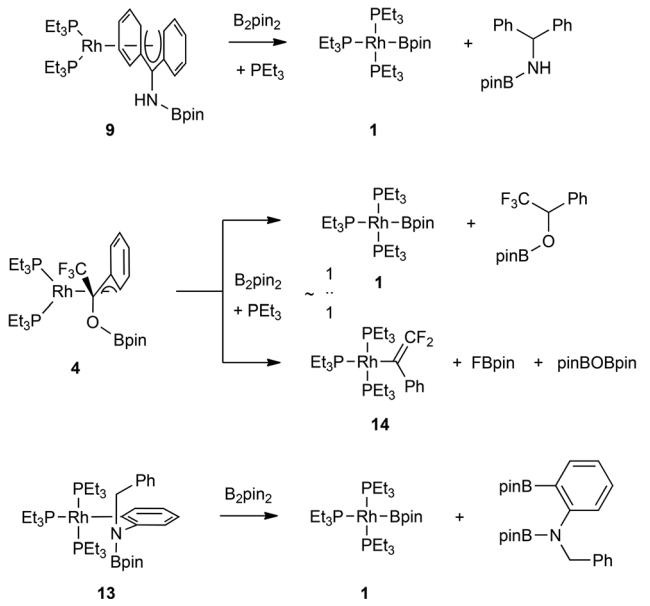

Scheme 5 Reactivity of complexes **9**, **4** and **13** towards B_2pin_2.

products of an imine[96] in a metal–boron single[97] bond are unprecedented. The reactions also confirm that a Rh–C and a N–B bond formation is favored over a Rh–N and a C–B bond formation. Overall, the results demonstrate that the insertion reactions into a Rh–B bond can lead to diverse products, and consecutive reactions such as C–H or C–F activation or CO insertion steps were also observed. Although no catalytic procedure reaction has been developed so far, the transformations might be of certain interest for the development of new borylation reactions in the future.

Experimental

[D_6]benzene, [D_8]toluene, [D_{12}]cyclohexane, cyclohexane, hexane, and hexamethyldisilane were dried by stirring over Na/K and then distilled. Complex [Rh(Bpin)(PEt_3)$_3$] (**1**) was prepared according to the literature.[51] The imines *N*-(diphenylmethylene)aniline,[98] *N*-(fluoren-9-ylidene)aniline,[99] and *N*-benzylidenehexan-1-amine[100] were prepared according to the literature. The NMR spectra were recorded at 300 K (if not stated otherwise) on a Bruker Avance 400, a Bruker DPX 300 or a Bruker Avance III 300 NMR spectrometer. The ^{1}H NMR chemical shifts were referenced to residual C_6D_5H at δ 7.16 ppm, [D_7]toluene at δ 2.09 ppm or [D_{11}]cyclohexane at δ 1.43 ppm. The $^{11}B\{^1H\}$ NMR spectra were referenced to external $BF_3{\cdot}OEt_2$ at δ 0.0 ppm, the ^{19}F NMR spectra to external $CFCl_3$ at δ 0.0 ppm, and the $^{31}P\{^1H\}$ NMR spectra to external H_3PO_4 at δ 0.0 ppm. In order to get a ^{2}H lock signal, C_6D_6 was introduced in the space between the glass NMR tubes and the PFA inliners, which contained the reaction mixture with hexamethyldisilane or cyclohexane as a solvent. Mass spectra were measured on a Micromass Q-Tof-2 instrument equipped with a Linden LIFDI source (Linden CMS GmbH). GC-MS spectra were measured on an Agilent 6890N gas-phase chromatograph (Agilent 19091S-433 Hewlett-Packard) and an Agilent 5973 Network mass selective detector at 70 eV. The microanalyses were obtained using a Euro EA HEKAtech elemental analyzer.

Treatment of [Rh(Bpin)(PEt_3)$_3$] (1) with acetophenone

A solution of [Rh(Bpin)(PEt_3)$_3$] (**1**) (39.5 mg, 68 μmol) in hexamethyldisilane (0.3 mL) in a PFA tube was treated with acetophenone (3.9 mg, 34 μmol). After 15 min the $^{31}P\{^1H\}$ NMR spectroscopic data of the reaction solution revealed the complete conversion of **1** and the formation of [Rh(H)(PEt_3)$_3$] (**2**) as well as of [Rh(OBpin)(PEt_3)$_3$] (**3**) in a ratio of **1** : **1**. The ^{1}H and $^{13}C\{^1H\}$ NMR spectroscopic data indicated the presence of (*E*)-(Ph)CH=CHBpin as the main product. The latter was identified by comparison with literature NMR data.[53] Analytical data for **3**: (Found: C, 48.07; H, 9.60. $C_{24}H_{57}BO_3P_3Rh$ requires C, 48.02; H, 9.57%); ^{1}H NMR (300.1 MHz, Me_6Si_2): δ = 2.06 (12H, m, CH_2), 1.83 (6H, m, CH_2), 1.61–1.45 (39H, m, CH_3) ppm. ^{11}B NMR (96.3 MHz, Me_6Si_2): δ = 22.8 ($\Delta\nu_{1/2} \approx$ 150 Hz) ppm. $^{13}C\{^1H\}$ NMR (75.5 MHz, C_6D_6): δ = 78.5 (*C*Me_2), 25.7 (CH_3), 21.3 (d, J_{PC} = 25 Hz, CH_2), 16.9 (t, J = 10 Hz, CH_2), 9.2 (CH_3) ppm. $^{31}P\{^1H\}$ NMR (121.5 MHz, Me_6Si_2): δ = 40.2 (1P, dt, J_{RhP} = 172 Hz, J_{PP} = 43 Hz), 21.4 (2P, dd, J_{RhP} = 142 Hz, J_{PP} = 43 Hz, J_{FP} = 8 Hz) ppm. MS (LIFDI, Me_6Si_2), *m*/*z*: 600 $[M]^+$.

Treatment of [Rh(Bpin)(PEt_3)$_3$] (1) with styrene

(a) A solution of [Rh(Bpin)(PEt_3)$_3$] (**1**) (43.7 mg, 75 μmol) in hexamethyldisilane (0.3 mL) in a PFA tube was treated with styrene (8.6 μL, 75 μmol). After 15 min the NMR spectroscopic data of the reaction solution revealed a quantitative conversion and the formation of [Rh(H)(PEt_3)$_3$] (**2**) as well as the formation of (*E*)-(Ph)CH=CHBpin. The latter was identified by comparison with literature NMR data.[53]

(b) A solution of [Rh(Bpin)(PEt_3)$_3$] (**1**) (28.6 mg, 49 μmol) in hexamethyldisilane (0.2 mL) in a PFA tube was treated with styrene (2.8 μL, 25 μmol). After 1 h the NMR spectroscopic data of the reaction solution revealed quantitative conversion and the formation of [Rh(H)(PEt_3)$_3$] (**2**) as well as the formation of (*E*)-(Ph)CH=C(Bpin)$_2$. The latter was identified by comparison with literature NMR data.[54]

Synthesis of [Rh{η^3-C(CF_3)(OBpin)C_6H_5}(PEt_3)$_2$] (4)

A solution of [Rh(Bpin)(PEt_3)$_3$] (**1**) (71.8 mg, 123 μmol) in hexamethyldisilane (0.3 mL) in a PFA tube was treated with α,α,α-trifluoroacetophenone (21.4 mg, 123 μmol). After 5 min at room temperature the volatiles were removed under vacuum to give a dark red oil. Yield 80.6 mg. ^{1}H NMR (300.1 MHz, Me_6Si_2): δ = 7.62 (2H, br s, CH_{ar}), 7.24 (1H, t, J_{HH} = 7 Hz, CH_{ar}), 7.10 (1H, br s, CH_{ar}), 6.34 (1H, br s, CH_{ar}), 2.28 (3H, m, CH_2), 2.10 (3H, m, CH_2), 1.70 (6H, m, CH_2), 1.60 (6H, s, CH_3), 1.58 (6H, s, CH_3), 1.49 (9H, dt, J_{RhH} = 15 Hz, J_{PH} = 8 Hz, CH_3), 0.94 (9H, dt, J_{RhH} = 15 Hz, J_{PH} = 7 Hz, CH_3) ppm. ^{11}B NMR (96.3 MHz, Me_6Si_2): δ = 22.5 ($\Delta\nu_{1/2} \approx$ 60 Hz) ppm. $^{13}C\{^1H\}$ NMR (75.5 MHz, Me_6Si_2): δ = 123.8 (CH_{ar}), 109.2 (q, J_{FC} = 276 Hz, CF_3), 82.4 (*C*Me_2), 65.3 (q, J_{FC} = 36 Hz, *C*CF_3), 25.1 (CH_3), 19.6 (d, J_{PC} = 23 Hz, CH_2), 18.2 (d, J_{PC} = 19 Hz, CH_2), 9.2 (CH_3),

9.1 (CH_3) ppm. The signals for the other aromatic carbon atoms were not observed. The resonances for the CF_3 and CCF_3 carbon atoms were confirmed by a ^{13}C–^{19}F-HMQC spectrum. $^{19}F\{^1H\}$ NMR (75.3 MHz, Me_6Si_2): δ = −57.4 (d, J_{PF} = 9 Hz) ppm. $^{31}P\{^1H\}$ NMR (121.5 MHz, Me_6Si_2): δ = 28.1 (dd, J_{RhP} = 257 Hz, J_{PP} = 36 Hz), 21.8 (ddq, J_{RhP} = 160 Hz, J_{PP} = 36 Hz, J_{FP} = 8 Hz) ppm. MS (LIFDI, Me_6Si_2), *m*/*z*: 640 $[M]^+$. The reaction solution always contained small amounts (5–10%) of $PhCH(OBpin)CF_3$, which was identified by comparison of the NMR data with data of an independently synthesized sample by treatment of α,α,α-trifluoroacetophenone with HBpin in C_6D_6 at room temperature (50% conversion after 9 d). Analytical data for $PhCH(OBpin)CF_3$: ^1H NMR (300.1 MHz, C_6D_6): δ = 7.38 (2H, m, CH_{ar}), 7.02 (3H, m, CH_{ar}), 5.58 (1H, q, J_{FH} = 7 Hz, CH), 0.98 (6H, s, CH_3), 0.93 (6H, s, CH_3) ppm. $^{13}C\{^1H\}$ NMR (75.5 MHz, Me_6Si_2): δ = 134.7 (C_{ar}), 129.6 (CH_{ar}), 128.7 (CH_{ar}), 128.3 (CH_{ar}), 124.4 (q, J_{FC} = 280 Hz, CF_3), 83.6 (CMe_2), 75.0 (q, J_{FC} = 33 Hz, CCF_3), 25.1 (CH_3), 25.0 (CH_3) ppm. $^{19}F\{^1H\}$ NMR (75.3 MHz, C_6D_6): δ = −78.4 (s) ppm. GC-MS, *m*/*z*: 302 [M], 287 $[M - CH_3]$.

Synthesis of *trans*-[Rh{C(O)C(CF$_3$)(Ph)OBpin}(CO)(PEt$_3$)$_2$] (5)

A solution of $[Rh(Bpin)(PEt_3)_3]$ (**1**) (113.9 mg, 195 μmol) in hexamethyldisilane (1.0 mL) in a PFA tube was treated with α,α,α-trifluoroacetophenone (34.0 mg, 195 μmol). After stirring for 30 min at room temperature, the volatiles were removed under vacuum. The residue was dissolved in hexamethyldisilane (0.7 mL) and the solution was filtered. After the filtrate was cooled to 77 K and degassed, the vessel was purged with CO. The dark red reaction mixture was then allowed to warm to room temperature. A yellow solid precipitated within 2 h, which was separated and washed with hexamethyldisilane (2 × 0.25 mL), hexane (2 × 0.25 mL) and dried *in vacuo*. Yield 81.0 mg (60%). (Found: C, 48.37; H, 6.88. $C_{28}H_{47}BF_3O_5P_2Rh$ requires C, 48.30; H, 6.80%); $\tilde{\nu}$ (ATR, diamond) 1952 (C≡O), 1478 (C═O), 903 cm^{-1}. ^1H NMR (300.1 MHz, C_6D_6): δ = 8.59 (2H, d, J_{HH} = 8 Hz, CH_{ar}), 7.09 (2H, td, J_{HH} = 7 Hz, J = 1 Hz, CH_{ar}), 6.97 (1H, tt, J_{HH} = 7 Hz, J = 1 Hz, CH_{ar}), 1.55 (18H, m, CH_2, CH_3), 1.24 (3H, m, CH_2), 0.94 (9H, m, CH_3), 0.76 (9H, m, CH_3), 0.63 (3H, m, CH_2) ppm. ^{11}B NMR (96.3 MHz, C_6D_6): δ = 15.3 ($\Delta\nu_{1/2} \approx 200$ Hz) ppm. $^{13}C\{^1H\}$ NMR (75.5 MHz, C_6D_6): δ = 296.1 (d, J_{RhC} = 42 Hz, C═O), 198.7 (d, J_{RhC} = 53 Hz, C≡O), 137.0 (C_{ar}), 128.8 (CH_{ar}), 128.3 (CH_{ar}), 128.3 (CH_{ar}), 124.4 (q, J_{FC} = 286 Hz, CF_3), 100.1 (q, J_{FC} = 23 Hz, CCF_3), 80.1 (CMe_2), 26.1 (CH_3), 26.0 (CH_3), 18.7 (d, J_{PC} = 24 Hz, CH_2), 17.9 (d, J_{PC} = 24 Hz, CH_2), 8.4 (CH_3) ppm. $^{19}F\{^1H\}$ NMR (75.3 MHz, C_6D_6): δ = −71.8 (d, J_{PF} = 4 Hz) ppm. $^{31}P\{^1H\}$ NMR (121.5 MHz, C_6D_6): δ = 21.8 (ddq, J_{PP} = 210 Hz, J_{RhP} = 141 Hz, J_{FP} = 4 Hz), 19.8 (dd, J_{PP} = 210 Hz, J_{RhP} = 141 Hz) ppm. Complex **5a** was prepared in a similar manner using ^{13}CO. Analytical data for **5a**: $\tilde{\nu}$ (ATR, diamond) 1906 (C≡O), 1445 (C═O), 885 cm^{-1}; $^{13}C\{^1H\}$ NMR (75.5 MHz, [D$_8$]toluene): δ = 296.1 (ddt, J_{RhC} = 42 Hz, J_{CC} = 34 Hz, J_{PC} = 12 Hz, C═O), 198.7 (ddt, J_{RhC} = 52 Hz, J_{CC} = 34 Hz, J_{PC} = 16 Hz, C≡O) ppm. The other data are similar to those for **5**. $^{31}P\{^1H\}$ NMR (121.5 MHz, [D$_8$]toluene): δ = 20.6 (ddm, J_{PP} = 210 Hz, J_{RhP} = 141 Hz), 17.9 (dddd, J_{PP} = 210 Hz, J_{RhP} = 141 Hz, J_{CP} = 16 Hz, J_{CP} = 13 Hz) ppm. The ^1H, ^{11}B and ^{19}F NMR data are identical to those for **6**.

Synthesis of [Rh{η^5-C$_{13}$H$_8$(OBpin)}(PEt$_3$)$_2$] (6)

A solution of $[Rh(Bpin)(PEt_3)_3]$ (**1**) (78.5 mg, 134 μmol) in hexamethyldisilane (0.6 mL) in a PFA tube was treated with fluoren-9-one (24.2 mg, 134 μmol). After stirring for 1 h at room temperature, the volatiles were removed under vacuum. The residue was extracted with hexane (3 × 1 mL). The extract was dried under vacuum to give a very air sensitive orange red powder. Yield 80.6 mg (93%). (Found: C, 57.36; H, 7.89. $C_{31}H_{50}BO_3P_2Rh$ requires C, 57.60; H, 7.80%); ^1H NMR (300.1 MHz, C_6D_6): δ = 7.61 (2H, d, J_{HH} = 8 Hz, CH_{ar}), 7.50 (2H, d, J_{HH} = 8 Hz, CH_{ar}), 7.13 (2H, t, J_{HH} = 7 Hz, CH_{ar}), 6.99 (2H, t, J_{HH} = 7 Hz, CH_{ar}), 1.59 (6H, m, q in the $^1H\{^{31}P\}$ spectrum, J_{HH} = 7 Hz, CH_2), 1.27 (6H, m, q in the $^1H\{^{31}P\}$ spectrum, J_{HH} = 7 Hz, CH_2), 0.94 (12H, s, CH_3), 0.84 (9H, m, t in the $^1H\{^{31}P\}$ spectrum, J_{HH} = 8 Hz, CH_3), 0.63 (9H, m, t in the $^1H\{^{31}P\}$ spectrum, J_{HH} = 7 Hz, CH_3) ppm. ^{11}B NMR (96.3 MHz, C_6D_6): δ = 22.7 ($\Delta\nu_{1/2} \approx 200$ Hz) ppm.$^{13}C\{^1H\}$ NMR (75.5 MHz, C_6D_6): δ = 120.7 (CH_{ar}), 119.6 (d, J = 2 Hz, CH_{ar}), 118.1(d, J = 3 Hz, CH_{ar}), 113.9 (CH_{ar}), 111.1 (br, C_{ar}), 102.3 (dm, J = 24 Hz, CO), 97.7 (q, J = 2 Hz, C_{ar}), 83.2 (CMe_2), 24.4 (CH_3), 20.2 (d, J_{PC} = 21 Hz, CH_2), 19.1 (d, J_{PC} = 23 Hz, CH_2), 8.2 (CH_3), 8.0 (CH_3) ppm.$^{31}P\{^1H\}$ NMR (121.5 MHz, Me_6Si_2): δ = 40.7 (dd, J_{RhP} = 254 Hz, J_{PP} = 43 Hz), 19.8 (dd, J_{RhP} = 204 Hz, J_{PP} = 44 Hz) ppm.

Synthesis of [Rh{η^3-C$_6$H$_5$═C(Ph)N(Ph)(Bpin)}(PEt$_3$)$_2$] (7)

A solution of $[Rh(Bpin)(PEt_3)_3]$ (**1**) (86.7 mg, 149 μmol) in hexamethyldisilane (0.7 mL) in a PFA tube was treated with *N*-(diphenylmethylene)aniline (38.2 mg, 149 μmol) to give a dark red solution. After stirring for 1 d a dark red solid precipitated at room temperature, which was separated and washed with hexamethyldisilane (0.2 mL) and dried *in vacuo*. Yield 87.0 mg (81%). (Found: C, 61.76; H, 8.03; N, 1.75. $C_{37}H_{57}BNO_2P_2Rh$ requires C, 61.42; H, 7.94; N, 1.94%); ^1H NMR (300.1 MHz, C_6D_6, major isomer): δ = 7.74 (2H, d, J_{HH} = 7 Hz, CH_{ar}), 7.67 (2H, d, J_{HH} = 7 Hz, CH_{ar}), 7.34–7.14 (4H, m, CH_{ar}), 6.98 (1H, br t, CH_{ar}), 6.89 (1H, t, J_{HH} = 7 Hz, CH_{ar}), 6.45 (1H, d, J = 8 Hz, CH_{ring}), 5.84 (1H, br m, CH_{ring}), 5.52 (1H, br t, CH_{ring}), 5.20 (1H, d, J = 6 Hz, CH_{ring}), 4.09 (1H, m, CH_{ring}), 1.54–0.82 (42H, m, CH_2, CH_3) ppm. ^1H NMR (300.1 MHz, C_6D_6, minor isomer): δ = 7.89 (2H, d, J_{HH} = 8 Hz, CH_{ar}), 7.82 (2H, d, J_{HH} = 7 Hz, CH_{ar}), 5.97 (1H, m, J = 6 Hz, CH_{ring}), 5.79 (1H, br t, CH_{ring}), 5.66 (1H, d, J = 8 Hz, CH_{ring}), 4.28 (1H, m, CH_{ring}) ppm. The signals for the other hydrogen atoms are obscured by signals of the major isomer. ^{11}B NMR (96.3 MHz, Me_6Si_2): δ = 25.2 ($\Delta\nu_{1/2} \approx 250$ Hz) ppm. $^{13}C\{^1H\}$ NMR (75.5 MHz, C_6D_6, major isomer): δ = 148.4 (C_{ar}), 143.6 (C_{ar}), 134.1 (t, J = 7 Hz, C═C), 129.0 (CH_{ar}), 128.1 (CH_{ar}), 127.9 (CH_{ar}), 124.2 (CH_{ar}), 121.5 (CH_{ar}), 121.5 (CH_{ar}), 112.6 (br s, CH_{ring}), 103.1 (br s, CH_{ring}), 99.6 (br s, CH_{ring}), 82.1 (CMe_2), 80.7 (br s, CH_{ring}), 66.2 (td, J_{PC} = 7 Hz, $J_{Rh,C}$ = 5 Hz, CH_{ring}), 25.0 (CH_3), 23.9 (CH_2), 21.1 (t, J = 11 Hz, CH_2), 8.9 (CH_3) ppm. The signal for one quaternary carbon atom of the enamine was not found. $^{31}P\{^1H\}$ NMR (121.5 MHz, Me_6Si_2, 300 K): δ = 31.8 (1P, d, J_{RhP} = 212 Hz,

major isomer), 30.5 (0.2P, d, J_{RhP} = 212 Hz, minor isomer) ppm. $^{31}P\{^1H\}$ NMR (121.5 MHz, [D$_8$]toluene, 273 K): δ = 31.8 (1P, d, J_{RhP} = 210 Hz, major product), 30.4 (0.3P, d, J_{RhP} = 209 Hz, minor isomer) ppm. $^{31}P\{^1H\}$ NMR (121.5 MHz, [D$_8$] toluene, 253 K): δ = ~32.0 (1P, br d, ~200 Hz, major isomer), 30.5 (0.3P, d, J_{RhP} = 209 Hz, minor isomer) ppm. $^{31}P\{^1H\}$ NMR (121.5 MHz, [D$_8$]toluene, 223 K): δ = 34.9 (br d, J_{RhP} ~ 210 Hz, major isomer), 30.6 (d, J_{RhP} = 208 Hz, minor isomer), 29.7 (br d, J_{RhP} ~ 210 Hz, major isomer) ppm. $^{31}P\{^1H\}$ NMR (121.5 MHz, [D$_8$]toluene, 203 K): δ = 35.5 (dd, J_{RhP} = 210 Hz, J_{PP} = 46 Hz, major isomer), 29.5 (dd, J_{RhP} = 213 Hz, J_{PP} = 46 Hz, major isomer) ppm. $^{31}P\{^1H\}$ NMR (121.5 MHz, [D$_8$]toluene, 333 K): δ = 26.1 (d, J_{RhP} = 212 Hz) ppm.

Synthesis of [Rh{(η^3-C$_{12}$H$_8$)N(Ph)(Bpin)}(PEt$_3$)$_2$] (8)

A solution of [Rh(Bpin)(PEt$_3$)$_3$] (**1**) (92.8 mg, 159 μmol) in hexamethyldisilane (0.7 mL) in a PFA tube was treated with *N*-(fluoren-9-ylidene)aniline (40.5 mg, 159 μmol). After 30 min the volatiles were removed under vacuum. The purple residue was washed with hexamethyldisilane (2 × 0.3 mL) and hexane (2 × 0.3 mL) and then dried *in vacuo* to give a purple solid. Yield 83.1 mg (80%). (Found: C, 61.71; H, 7.84; N, 1.72. C$_{37}$H$_{55}$BNO$_2$P$_2$Rh requires C, 61.59; H, 7.68; N, 1.94%); ^1H NMR (300.1 MHz, [D$_8$]toluene): δ = 8.01 (1H, br d, J_{HH} = 8, CH), 7.68 (1H, br s, CH), 7.47–6.95 (7H, m, CH), 6.89 (1H, br s, CH), 6.78 (1H, t, J_{HH} = 7 Hz, CH), 6.22 (1H, br s, CH), 5.98 (1H, br s, CH$_{fluorene}$), 1.29–1.02 (24H, m, CH$_2$, CH$_3$), 0.74 (18H, m, CH$_3$) ppm. ^{11}B NMR (96.3 MHz, C$_6$D$_6$): δ = 24.8 ($\Delta\nu_{1/2}$ ≈ 500 Hz) ppm. $^{13}C\{^1H\}$ NMR (75.5 MHz, [D$_8$]toluene): δ = 149.1 (C$_{ar}$), 139.8 (NC$_{fluorene}$), 131.9 (d, *J* = 7 Hz, CH$_{fluorene}$), 129.6 (CH), 128.5 (CH), 123.7 (CH), 122.5 (CH), 121.3 (CH), 118.9 (CH), 117.3 (CH), 116.9 (CH), 109.9 (C$_{fluorene}$), 98.6 (br s, CH$_{fluorene}$), 97.8 (br s, C$_{fluorene}$), 87.0 (br s, C$_{fluorene}$), 82.3 (*C*Me$_2$), 70.6 (br s, CH$_{fluorene}$), 25.4 (CH$_3$), 24.3 (CH$_3$), 20.1 (d, J_{PC} = 11 Hz, CH$_2$), 8.2 (CH$_3$) ppm. The signal for one quarternary carbon atom was not found. $^{31}P\{^1H\}$ NMR (121.5 MHz, C$_6$D$_6$, 300 K): δ = 34.2 (br d, J_{RhP} = 215 Hz) ppm. $^{31}P\{^1H\}$ NMR (121.5 MHz, [D$_8$]toluene, 243 K): δ = 35.0 (1P, d, J_{RhP} = 213 Hz, major isomer), 33.2 (0.55P, d, J_{RhP} = 210 Hz, minor isomer) ppm. $^{31}P\{^1H\}$ NMR (121.5 MHz, [D$_8$]toluene, 203 K): δ = 35.0 (1P, d, J_{RhP} = 213 Hz, major isomer), 33.2 (0.85P, d, J_{RhP} = 210 Hz, minor isomer) ppm.

Synthesis of [Rh{CPh$_2$N(H)(Bpin)}(PEt$_3$)$_2$] (9) and 9′

(a) A solution of [Rh(Bpin)(PEt$_3$)$_3$] (**1**) (67.2 mg, 115 μmol) in hexamethyldisilane (0.6 mL) in a PFA tube was treated slowly with benzophenone imine (20.8 mg, 115 μmol) while stirring. After 5 min at room temperature the NMR spectroscopic data of the reaction solution revealed a quantitative conversion of **1** and the formation of **9** and **9′** in a ratio of 3 : 1 (according to the $^{31}P\{^1H\}$ NMR at 188 K) and PEt$_3$. Analytical data for **9**: ^1H NMR (300.1 MHz, Me$_6$Si$_2$): δ = 7.66 (4H, d, J_{HH} = 8 Hz, 4H, CH$_{ar}$), 7.49 (4H, t, J_{HH} = 8 Hz, CH$_{ar}$), 7.25 (2H, t, J_{HH} = 7 Hz, CH$_{ar}$), 3.08 (1H, d, J_{PH} = 7, NH), 1.67 (12H, m, CH$_2$), 1.57–1.21 (30H, m, CH$_3$) ppm. ^{11}B NMR (96.3 MHz, Me$_6$Si$_2$): δ = 24.6 ($\Delta\nu_{1/2}$ ≈ 400 Hz) ppm. $^{13}C\{^1H\}$ NMR (75.5 MHz, C$_6$D$_6$): δ = 135.1 (br s, C$_{ar}$), 129.0 (CH$_{ar}$), 123.6 (CH$_{ar}$), 118.1 (br s, CH$_{ar}$), 81.3 (*C*Me$_2$), 68.7 (dm, J_{RhC} = 42 Hz, CN), 25.0 (CH$_3$), 19.7 (d, J_{PC} = 21 Hz, CH$_2$), 18.0 (d, J_{PC} = 17 Hz, CH$_2$), 9.3 (CH$_3$) ppm. $^{31}P\{^1H\}$ NMR (121.5 MHz, Me$_6$Si$_2$, 300 K): δ = 22.3 (dd, J_{RhP} = 163 Hz, J_{PP} = 32 Hz), 18.7 (dd, J_{RhP} = 262 Hz, J_{PP} = 32 Hz) ppm. MS (LIFDI, Me$_6$Si$_2$), *m*/*z*: 647 [M]$^+$. Analytical data for **9′**: $^{31}P\{^1H\}$ NMR (121.5 MHz, [D$_8$]toluene, 253 K): δ = 13.8 (br d, *J* = 145 Hz) ppm. $^{31}P\{^1H\}$ NMR (121.5 MHz, [D$_8$]toluene, 188 K): δ = 23.7 (1P, dt, J_{RhP} = 119 Hz, J_{PP} = 37 Hz), 13.1 (2P, dd, J_{RhP} = 155 Hz, J_{PP} = 37 Hz) ppm.

(b) A solution of [Rh(Bpin)(PEt$_3$)$_3$] (**1**) (39.7 mg, 68 μmol) in hexamethyldisilane (0.2 mL) in a PFA tube was treated with benzophenone imine (12.2 mg, 68 μmol) without stirring. After 5 min at room temperature the volatiles were removed under vacuum and the dark red oil was redissolved in hexamethyldisilane. The NMR spectroscopic data revealed a quantitative conversion of **1** and the formation of **9** and [Rh{N=CPh$_2$}(PEt$_3$)$_3$] (**10**) in a ratio of 100 : 6. Complex **10** was identified by its NMR data.[76]

(c) A solution of [Rh(Bpin)(PEt$_3$)$_3$] (**1**) (11.7 mg, 20 μmol) in hexamethyldisilane (0.4 mL) in a PFA tube was treated slowly with benzophenone imine (3.6 mg, 20 μmol). The NMR spectroscopic data of the reaction solution revealed a quantitative formation of **9** after 5 min at room temperature and the formation of **9** and [Rh{N=CPh$_2$}(PEt$_3$)$_3$] (**10**) in a ratio of 10 : 1 after 4 h. Complex **10** was identified by its NMR data.[76]

Synthesis of [Rh[η^3-CH{N(C$_6$H$_{13}$)Bpin}C$_6$H$_5$](PEt$_3$)$_2$] (11)

A solution of [Rh(Bpin)(PEt$_3$)$_3$] (**1**) (74.8 mg, 128 μmol) in hexamethyldisilane (0.4 mL) in a PFA tube was treated with *N*-benzylidenehexan-1-amine (24.2 mg, 128 μmol). After 5 min at room temperature the volatiles were removed under vacuum to give a red oil. Yield 85.1 mg of crude product, which contains 2% impurities. ^1H NMR (300.1 MHz, Me$_6$Si$_2$): δ = 7.45 (2H, br s, CH$_{ar}$), 6.99 (1H, t, J_{HH} = 7 Hz, CH$_{ar}$), 6.34 (2H, br s, CH$_{ar}$), 4.15 (1H, t, J_{PH} = 5 Hz, NCH), 3.66 (1H, dt, J_{HH} = 13 Hz, J_{HH} = 7 Hz, NCH$_2$), 3.37 (1H, dt, J_{HH} = 13 Hz, J_{HH} = 6 Hz, NCH$_2$), 2.09 (6H, m, t in the $^1H\{^{31}P\}$ spectrum, J_{HH} = 7 Hz, CH$_2$), 2.09 (6H, m, CH$_2$), 1.90–1.28 (23H, m, CH$_2$, CH$_3$), 1.50 (12H, s, CH$_2$), 1.20 (9H, m, CH$_3$) ppm. ^{11}B NMR (96.3 MHz, Me$_6$Si$_2$): δ = 24.5 ($\Delta\nu_{1/2}$ ≈ 400 Hz) ppm. $^{13}C\{^1H\}$ NMR (75.5 MHz, Me$_6$Si$_2$): δ = 121.7 (CH$_{ar}$), 81.6 (*C*Me$_2$), 65.5 (dd, J_{RhC} = 42 Hz, J_{PC} = 12 Hz, CHN), 52.8 (NCH$_2$), 32.5 (CH$_2$), 30.6 (CH$_2$), 27.1 (CH$_2$), 25.7 (CH$_3$), 23.5 (CH$_2$), 21.6 (d, $J_{P,C}$ = 20 Hz, CH$_2$), 19.0 (d, J_{PC} = 16 Hz, CH$_2$), 14.7 (CH$_3$), 9.2 (CH$_3$) ppm. The signals for the other aromatic carbon atoms were not observed. $^{31}P\{^1H\}$ NMR (121.5 MHz, Me$_6$Si$_2$): δ = 25.8 (dd, J_{RhP} = 270 Hz, J_{PP} = 26 Hz), 21.7 (dd, J_{RhP} = 168 Hz, J_{PP} = 26 Hz) ppm. MS (LIFDI, Me$_6$Si$_2$), *m*/*z*: 655 [M]$^+$.

Synthesis of [Rh{(C$_6$H$_4$)-*o*-N(Bpin)(CH$_2$Ph)}(PEt$_3$)$_3$] (13)

A solution of [Rh(Bpin)(PEt$_3$)$_3$] (**1**) (91.9 mg, 157 μmol) in hexamethyldisilane (0.6 mL) in a PFA tube was treated with *N*-benzylideneaniline (28.5 mg, 157 μmol). The solution turned red immediately. The NMR spectroscopy data revealed the formation of **12**. After 10 min the solution turned orange. After

1 h the volatiles were removed under vacuum. The residue was washed with cold hexane (0.2 mL) and dried *in vacuo* to give **13** as a very air sensitive yellow solid. Yield 111.0 mg (92%). Analytical data for **13**: (Found: C, 58.39; H, 8.96; N, 1.63. $C_{37}H_{68}BNO_2P_3Rh$ requires C, 58.05; H, 8.95; N, 1.83%); ^{1}H NMR (300.1 MHz, C_6D_6): δ = 8.03 (1H, dd, J_{HH} = J_{PH} = 7 Hz, CH_{ar}), 7.67 (1H, d, J_{HH} = 8 Hz, CH_{ar}), 7.57 (2H, d, J_{HH} = 8 Hz, CH_{ar}), 7.15 (2H, m, CH_{ar}), 7.09 (1H, m, CH_{ar}), 6.96 (1H, t, J_{HH} = 7 Hz, CH_{ar}), 6.86 (1H, t, J_{HH} = 7 Hz, CH_{ar}), 6.30 (2H, s, NCH_2), 1.38 (6H, m, q in the ^{1}H{^{31}P} spectrum, J_{HH} = 7 Hz, CH_2), 1.27 (12H, m, q in the ^{1}H{^{31}P} spectrum, J_{HH} = 8 Hz, CH_2), 1.00 (12H, s, CH_3), 0.96 (9H, m, t in the ^{1}H{^{31}P} spectrum, J_{HH} = 8 Hz, CH_3), 0.86 (18H, m, t in the ^{1}H{^{31}P} spectrum, J_{HH} = 8 Hz, CH_3) ppm. ^{11}B NMR (96.3 MHz, Me_6Si_2): δ = 24.8 ($\Delta\nu_{1/2} \approx$ 250 Hz) ppm. ^{13}C{^{1}H} NMR (75.5 MHz, cyclohexane): δ = 164.8 (ddt, J_{RhC} = 77 Hz, J_{PC} = 27 Hz, J_{PC} = 17 Hz, RhC_{ar}), 153.1 (m, C_{ar}), 146.8 (C_{ar}), 141.7 (CH_{ar}), 141.4 (t, J_{PC} = 4 Hz, CH_{ar}), 127.6 (CH_{ar}), 126.9 (CH_{ar}), 126.2 (m, CH_{ar}), 125.0 (CH_{ar}), 120.3 (d, t, J_{PC} = 4 Hz, CH_{ar}), 81.7 (CMe_2), 53.4 (NCH_2), 25.8 (CH_3), 19.9 (d, J_{PC} = 15 Hz, CH_2), 18.9 (d, J_{PC} = 10 Hz, CH_2), 8.8 (CH_3), 8.7 (CH_3) ppm. ^{31}P{^{1}H} NMR (121.5 MHz, Me_6Si_2): δ = 14.7 (1P, dt, J_{RhP} = 115 Hz, J_{PP} = 34 Hz), 8.8 (2P, dd, J_{RhP} = 159 Hz, J_{PP} = 34 Hz) ppm. Analytical data for **12**: ^{1}H NMR (300.1 MHz, Me_6Si_2): δ = 8.39 (d, J_{HH} = 8 Hz, 2H, CH_{ar}), 7.62–7.39 (m, 4H, CH_{ar}), 7.21 (m, 1H, CH_{ar}), 7.13 (m, 1H, CH_{ar}), 6.44 (m, 2H, CH_{ar}), 4.87 (dd, J_{PH} = 7 Hz, J = 3 Hz, 1H, NCH) ppm. The signals for the ethyl and methyl groups are obscured by signals of **1** and **13**. ^{31}P{^{1}H} NMR (121.5 MHz, Me_6Si_2): δ = 24.2 (dd, J_{RhP} = 275 Hz, J_{PP} = 27 Hz), 22.8 (dd, J_{RhP} = 170 Hz, J_{PP} = 27 Hz) ppm.

Treatment of [Rh{$CPh_2N(H)(Bpin)$}(PEt_3)$_2$] (9) and 9′ with B_2pin_2

B_2pin_2 (15.8 mg, 62 μmol) was added in a PFA tube to a solution of complex **9** in cyclohexane (0.3 mL), which was prepared *in situ* from [Rh(Bpin)(PEt_3)$_3$] (**1**) (33.0 mg, 57 μmol) and benzophenone imine (10.3 mg, 57 μmol). After 4 h at room temperature the NMR spectroscopic data of the reaction solution revealed the complete consumption of **9** and the quantitative formation of [Rh(Bpin)(PEt_3)$_3$] (**1**) as well as the formation of $Ph_2CHN(H)Bpin$ as the main product. Analytical data for $Ph_2CHN(H)Bpin$: ^{1}H NMR (300.1 MHz, [D_{12}]cyclohexane): δ = 7.61 (4H, d, J_{HH} = 8 Hz, CH_{ar}), 7.49–7.34 (6H, m, CH_{ar}), 6.26 (1H, s, CH), 1.30 (12H, s, CH_3) ppm. The signal for *N*-bound hydrogen was not observed. ^{11}B NMR (96.3 MHz, [D_{12}]cyclohexane): δ = 26.2 ($\Delta\nu_{1/2} \approx$ 550 Hz) ppm. ^{13}C{^{1}H} NMR (75.5 MHz, cyclohexane): δ = 144.5 (C_{ar}), 129.3 (CH_{ar}), 127.6 (CH_{ar}), 126.3 (CH_{ar}), 82.0 (CMe_2), 61.6 (NCH), 24.6 (CH_3) ppm. GC-MS, *m*/*z*: 309 [M], 294 [M − CH_3].

Treatment of [Rh{η^3-$C(CF_3)(OBpin)C_6H_5$}(PEt_3)$_2$] (4) with B_2pin_2

B_2pin_2 (19.6 mg, 77 μmol) was added in a PFA tube to a solution of complex **4** in cyclohexane (0.3 mL), which was prepared *in situ* from [Rh(Bpin)(PEt_3)$_3$] (**1**) (40.9 mg, 70 μmol) and α,α,α-trifluoroacetophenone (12.2 mg, 70 μmol). After 3 d at room temperature the ^{31}P{^{1}H} NMR spectroscopic data of the reaction solution revealed the complete conversion of **4** and the formation of [Rh(Bpin)(PEt_3)$_3$] (**1**) and [Rh{$C(=CF_2)Ph$}(PEt_3)$_3$] (**14**) in a ratio of approximately 1 : 1. The ^{19}F{^{1}H} NMR spectrum shows the resonances of **14**, FBpin, $PhCH(OBpin)CF_3$ and an unknown product at δ −66.5 ppm in a ratio of 1 : 1.5 : 0.5 : 1. Furthermore, $PhCH(OBpin)CF_3$ as well as pinBOBpin were identified by GC-MS measurements. Analytical data for **14**: ^{19}F{^{1}H} NMR (75.3 MHz, Me_6Si_2): δ = −75.1 (dm, J_{FF} = 73 Hz), −69.3 (ddq, J_{FF} = 73 Hz, J_{PF} = 24 Hz, J_{PF} = J_{RhF} = 4 Hz,) ppm. ^{31}P{^{1}H} NMR (121.5 MHz, Me_6Si_2): δ = 20.1 (1P, dtdd, J_{RhP} = 128 Hz, J_{PP} = 37 Hz, J_{FP} = 24 Hz, J_{FP} = 6 Hz), 11.6 (2P, ddt, J_{RhP} = 148 Hz, J_{PP} = 37 Hz, J_{FP} = 5 Hz) ppm. The signals of **14** in the ^{1}H NMR spectrum are obscured by the signals of **1**. MS (LIFDI, cyclohexane), *m*/*z*: 478 [M − PEt_3]$^+$.

Treatment of [Rh{(C_6H_4)-*o*-$N(Bpin)(CH_2Ph)$}(PEt_3)$_3$] (13) with B_2pin_2

A mixture of [Rh{(C_6H_4)-*o*-$N(Bpin)(CH_2C_6H_5)$}(PEt_3)$_3$] (**13**) (18.2 mg, 24 μmol) and B_2pin_2 (9.0 mg, 36 μmol) in [D_{12}]cyclohexane (0.2 mL) in a PFA tube was heated to 50 °C for 16 h. The NMR spectroscopic data of the reaction solution revealed the quantitative consumption of **13** and the formation of [Rh(Bpin)(PEt_3)$_3$] (**1**) and $PhCH_2N(Bpin)(C_6H_4$-*o*-Bpin). Analytical data for $PhCH_2N(Bpin)(C_6H_4$-*o*-Bpin): ^{1}H NMR (300.1 MHz, [D_{12}]cyclohexane): δ = 7.97 (1H, dd, J_{HH} = 7 Hz, J_{HH} = 2 Hz, CH_{ar}), 7.36–7.17 (6H, m, CH_{ar}), 7.13 (1H, t, J_{HH} = 7 Hz, CH_{ar}), 6.87 (1H, d, J_{HH} = 8 Hz, CH_{ar}), 4.62 (2H, s, CH_2), 1.34 (12H, s, CH_3), 1.32 (12H, m, CH_3) ppm. ^{11}B NMR (96.3 MHz, [D_{12}]cyclohexane): δ = 28.9 (CB), 24.6 (NB) ppm. ^{13}C{^{1}H} NMR (75.5 MHz, [D_{12}]cyclohexane): δ = 152.3 (C_{ar}), 141.8 (C_{ar}), 137.4 (CH_{ar}), 131.2 (CH_{ar}), 129.9 (CH_{ar}), 129.1 (CH_{ar}), 128.1 (CH_{ar}), 126.6 (CH_{ar}), 124.7 (CH_{ar}), 83.1 (CMe_2), 82.7 (CMe_2), 56.3 (CH_2), 25.0–27.0 (CH_3) ppm. The signal for the boron-bound carbon atom was not observed.

Structure determination of complexes 4, 5, 6, 7, 8, and 13

Purple crystals of **4**, red crystals of **6**, dark red crystals of **7**, deep purple crystals of **8**, and orange crystals of **12** precipitated from hexane solutions at −30 °C. Yellow crystals of **6** were obtained by crystallization from a low concentrated reaction solution of hexamethyldisilane. The diffraction data were collected on a STOE IPDS 2θ diffractometer at 100 K, except for complex **5** for which the data were collected at 90 K. Crystallographic data are depicted in Table 7. The structures were solved by direct methods (SHELXS-97[101] and SIR97[103]) and were refined with the full-matrix least-squares method on F^2 (SHELX-97 and SHELXL-2013).[101,102] Complex **6** shows disorder of one ethyl group. The orientational disorder was treated using rigid bond restraints (DELU) and a linear restraint (ISOR) for the ethyl group. A SQUEEZE refinement was applied for complex **13** for which the remaining electron density (*ca.* 2 electrons) did not allow an appropriate disordered model.

The hydrogen atoms were placed at the calculated positions and were refined by using a riding model.

Table 7 Crystallographic data

Compound	4	5	6	7	8	13
Empirical formula	$C_{26}H_{47}BF_3O_3P_2Rh$	$C_{28}H_{47}BF_3O_5P_2Rh$	$C_{31}H_{50}BO_3P_2Rh$	$C_{37}H_{57}BNO_2P_2Rh$	$C_{37}H_{55}BNO_2P_2Rh$	$C_{37}H_{68}BNO_2P_3Rh$
Formula weight	640.30	696.32	646.37	723.50	721.48	765.55
Crystal size (mm^3)	0.33 × 0.30 × 0.28	0.40 × 0.28 × 0.10	0.26 × 0.13 × 0.11	0.36 × 0.12 × 0.03	0.20 × 0.14 × 0.06	0.48 × 0.29 × 0.19
Wavelength (Å)	0.71073	0.71073	0.71073	0.71073	0.71073	0.71073
Crystal system	Monoclinic	Monoclinic	Orthorhombic	Monoclinic	Monoclinic	Monoclinic
Space group	$P2_1/c$	$P2_1/c$	$Pna2_1$	$P2_1/c$	$P2_1/n$	$C2/c$
a (Å)	16.1641(4)	10.4240(5)	24.5391(5)	19.0638(3)	15.1541(5)	42.3611(15)
b (Å)	10.6262(2)	29.0136(13)	10.0402(2)	20.0967(4)	13.2907(5)	10.5311(2)
c (Å)	19.1733(4)	13.0004(6)	13.0353(3)	20.5505(4)	18.0052(6)	23.6156(8)
β (°)	112.801(2)	124.428(3)		107.6360(10)	95.441(2)	120.338(3)
V ($Å^3$)	3035.91(12)	3243.1(3)	3211.60(12)	7503.3(2)	3610.1(2)	9092.5(5)
Z	4	4	4	8	4	8
Calculated density ($Mg\ m^{-3}$)	1.401	1.426	1.337	1.281	1.327	1.118
μ (Mo-Kα) (mm^{-1})	0.711	0.677	0.660	0.572	0.594	0.508
θ range (°)	2.10–29.50	2.36–26.76	2.03–28.32	4.63–26.85	3.27–29.23	4.67–26.00
Reflections collected	51 321	23 758	29 371	91 569	35 936	46 376
Independent reflections	8454	6630	7952	15 810	9707	8863
R_{int}	0.0399	0.0872	0.0681	0.0527	0.0961	0.0983
Goodness-of-fit on F^2	0.838	1.017	0.836	1.039	0.943	1.040
Completeness to max. θ	99.9%	97.1%	99.5%	98.0%	98.9%	99.4%
R_1, ωR_2 on all data	0.0301, 0.0471	0.0679, 0.1089	0.0424, 0.0630	0.0501, 0.0850	0.0840, 0.0777	0.0515, 0.1145
R_1, ωR_2 [$I_0 > 2\sigma(I_0)$]	0.0211, 0.0464	0.0479, 0.1021	0.0307, 0.0611	0.0352, 0.0808	0.0462, 0.0700	0.0406, 0.1089
Reflect. with [$I_0 > 2\sigma(I_0)$]	6623	5171	6246	12 772	6766	7377
Largest diff. peak, hole (e A^{-3})	0.506/−0.802	0.864/−1.556	0.564/−0.843	0.798/−1.178	0.716/−0.684	0.831/−1.116
CCDC	977662	977663	977664	977665	977666	977667

Acknowledgements

We acknowledge the Cluster of Excellence "Unifying Concepts in Catalysis", funded by the Deutsche Forschungsgemeinschaft, for financial support.

Notes and references

1 H. Braunschweig, *Angew. Chem., Int. Ed.*, 1998, **37**, 1786; H. Braunschweig, *Angew. Chem.*, 1998, **110**, 1882.
2 G. J. Irvine, M. G. Lesley, T. B. Marder, N. C. Norman, C. R. Rice, E. G. Robins, W. R. Roper, G. R. Whittell and L. J. Wright, *Chem. Rev.*, 1998, **98**, 2685.
3 H. Braunschweig, C. Kollann and D. Rais, *Angew. Chem., Int. Ed.*, 2006, **45**, 5254; H. Braunschweig, C. Kollann and D. Rais, *Angew. Chem.*, 2006, **118**, 5380.
4 H. Braunschweig and M. Colling, *Coord. Chem. Rev.*, 2001, **223**, 1.
5 H. Braunschweig, R. D. Dewhurst and A. Schneider, *Chem. Rev.*, 2010, **110**, 3924.
6 S. Aldridge and D. L. Coombs, *Coord. Chem. Rev.*, 2004, **248**, 535.
7 I. Beletskaya and A. Pelter, *Tetrahedron*, 1997, **53**, 4957.
8 T. B. Marder and N. C. Norman, *Top. Catal.*, 1998, **5**, 63.
9 H. Wadepohl, *Angew. Chem., Int. Ed. Engl.*, 1997, **36**, 2441; H. Wadepohl, *Angew. Chem.*, 1997, **109**, 2547.
10 J. F. Hartwig, *Chem. Soc. Rev.*, 2011, **40**, 1992.
11 L. Dang, Z. Lin and T. B. Marder, *Chem. Commun.*, 2009, 3987.
12 I. A. I. Mkhalid, J. H. Barnard, T. B. Marder, J. M. Murphy and J. F. Hartwig, *Chem. Rev.*, 2010, **110**, 890.
13 D. L. Kays and S. Aldridge, *Struct. Bonding*, 2008, **130**, 29.
14 R. T. Baker and J. C. Calabrese, *J. Am. Chem. Soc.*, 1993, **115**, 4367.
15 D. Männig and H. Nöth, *Angew. Chem., Int. Ed. Engl.*, 1985, **24**, 878; D. Männig and H. Nöth, *Angew. Chem.*, 1985, **97**, 854.
16 D. A. Evans and G. C. Fu, *J. Org. Chem.*, 1990, **55**, 2280.
17 K. Burgess, W. A. v. d. Donk, S. A. Westcott, T. B. Marder, R. T. Baker and J. C. Calabrese, *J. Am. Chem. Soc.*, 1992, **114**, 9350.
18 D. G. Mussaev, A. M. Mebel and K. Morokuma, *J. Am. Chem. Soc.*, 1994, **116**, 10693.
19 S. A. Westcott and T. B. Marder, *Organometallics*, 1993, **12**, 975.
20 C. Pubill-Ulldemolins, M. Poyatos, C. Bo and E. Fernández, *Dalton Trans.*, 2013, **42**, 746.
21 L. S. Sewell, A. B. Chaplin and A. S. Weller, *Dalton Trans.*, 2011, **40**, 7499.
22 T. Braun, M. Ahijado-Salomon, K. Altenhöner, M. Teltewskoi and S. Hinze, *Angew. Chem., Int. Ed.*, 2009, **48**, 1818; T. Braun, M. Ahijado-Salomon, K. Altenhöner, M. Teltewskoi and S. Hinze, *Angew. Chem.*, 2009, **121**, 1850.
23 K. B. Morgan, S. P. Miller and J. P. Morken, *J. Am. Chem. Soc.*, 2003, **125**, 8702.

24 P. Nguyen, R. B. Coapes, A. D. Woodward, N. J. Taylor, J. M. Burke, J. A. K. Howard and T. B. Marder, *J. Organomet. Chem.*, 2002, **625**, 77.
25 J. F. Hartwig, K. S. Cook, M. Hapke, C. D. Incarvito, Y. Fan, C. E. Webster and M. B. Hall, *J. Am. Chem. Soc.*, 2005, **127**, 2538.
26 S. Shimada, A. S. Batsanov, J. A. K. Howard and T. B. Marder, *Angew. Chem., Int. Ed.*, 2001, **40**, 2168; S. Shimada, A. S. Batsanov, J. A. K. Howard and T. B. Marder, *Angew. Chem.*, 2001, **113**, 2226.
27 W. H. Lam, K. C. Lam, Z. Lin, S. Shimada, R. N. Perutz and T. B. Marder, *Dalton Trans.*, 2004, 1556.
28 C. S. Wei, C. A. Jiménez-Hoyos, M. F. Videa, J. F. Hartwig and M. B. Hall, *J. Am. Chem. Soc.*, 2010, **132**, 3078.
29 J.-Y. Cho, C. N. Iverson and M. R. Smith III, *J. Am. Chem. Soc.*, 2000, **122**, 12868.
30 K. Mertins, A. Zapf and M. Beller, *J. Mol. Catal. A: Chem.*, 2003, **207**, 21.
31 H. Chen, S. Schlecht, T. C. Semple and J. F. Hartwig, *Science*, 2000, **287**, 1995.
32 R. T. Baker, P. Nguyen, T. B. Marder and S. A. Westcott, *Angew. Chem., Int. Ed. Engl.*, 1995, **34**, 1336; R. T. Baker, P. Nguyen, T. B. Marder and S. A. Westcott, *Angew. Chem.*, 1995, **107**, 1451.
33 C. Dai, E. G. Robins, A. J. Scott, W. Clegg, D. S. Yufit, J. A. K. Howard and T. B. Marder, *Chem. Commun.*, 1998, 1983.
34 P. Nguyen, R. B. Coapes, A. D. Woodward, N. J. Taylor, J. M. Burke, J. A. K. Howard and T. B. Marder, *J. Organomet. Chem.*, 2002, **652**, 77.
35 J. Ramírez, A. M. Sagarra and E. Fernández, *Tetrahedron: Asymmetry*, 2005, **16**, 1289.
36 A. Bonet, C. Pubill-Ulldemolins, C. Bo, H. Gulyás and E. Fernández, *Angew. Chem., Int. Ed.*, 2011, **50**, 7158; A. Bonet, C. Pubill-Ulldemolins, C. Bo, H. Gulyás and E. Fernández, *Angew. Chem.*, 2011, **123**, 7296.
37 A. Appel, T. M. Cameron, C. A. G. Carter, M. K. J. Gagnon, G. Mann, R. T. Baker, D. J. Harrison, C. M. Vogels and S. A. Westcott, *Contemp. Boron Chemistry*, 2000, 407.
38 N. Miyaura and A. Suzuki, *Chem. Rev.*, 195, **95**, 2457.
39 T. Ohmura, T. Awano and M. Suginome, *Chem. Lett.*, 2009, **38**, 664.
40 R. Smoum, A. Rubinstein, V. M. Dembitsky and M. Srebnik, *Chem. Rev.*, 2012, **112**, 4156.
41 W. Yang, X. Gao and B. Wang, *Med. Res. Rev.*, 2003, **23**, 346.
42 C. A. G. Carter, C. M. Vogels, D. J. Harrison, M. K. J. Gagnon, D. W. Norman, R. F. Langler, R. T. Baker and S. A. Westcott, *Organometallics*, 2001, **20**, 2130.
43 G. Mann, K. D. John and R. T. Baker, *Org. Lett.*, 2000, **2**, 2105.
44 T. M. Cameron, R. T. Baker and S. A. Westcott, *Chem. Commun.*, 1998, 2395.
45 V. P. Ananikov, R. Szilagyi, K. Morokuma and D. G. Musaev, *Organometallics*, 2005, **24**, 1938.
46 D. S. Laitar, E. Y. Tsui and J. P. Sadighi, *J. Am. Chem. Soc.*, 2006, **128**, 11036.
47 M. L. McIntosh, C. M. Moore and T. B. Clark, *Org. Lett.*, 2010, **12**, 1996.
48 C. Kleeberg, E. Feldmann, E. Hartmann, D. J. Vyas and M. Oestreich, *Chem.–Eur. J.*, 2011, **17**, 13538.
49 D. S. Laitar, P. Müller and J. P. Sadighi, *J. Am. Chem. Soc.*, 2005, **127**, 17196.
50 M. Teltewskoi, J. A. Panetier, S. A. Macgregor and T. Braun, *Angew. Chem., Int. Ed.*, 2010, **49**, 3947; M. Teltewskoi, J. A. Panetier, S. A. Macgregor and T. Braun, *Angew. Chem.*, 2010, **122**, 4039.
51 M. Teltewskoi, S. Kalläne and T. Braun, *Eur. J. Inorg. Chem.*, 2013, **33**, 5762.
52 M. Murata, S. Wantanabe and Y. Masuda, *Tetrahedron Lett.*, 1999, **40**, 2585.
53 I. A. I. Mkhalid, R. B. Coapes, S. N. Edes, D. N. Coventry, F. E. S. Souza, R. L. Thomas, J. J. Hall, S.-W. Bi, Z. Lin and T. B. Marder, *Dalton Trans.*, 2008, 1055.
54 J. Takaya, N. Kirai and N. Iwasawa, *J. Am. Chem. Soc.*, 2011, **133**, 12980.
55 G. A. Slough, R. Hayashi, J. R. Ashbaugh, S. L. Shamblin and A. M. Aukamp, *Organometallics*, 1994, **13**, 890.
56 P. Zhao and J. F. Hartwig, *Organometallics*, 2008, **27**, 4749.
57 J. R. Bleeke, E. Donnay and N. P. Rath, *Organometallics*, 2002, **21**, 4099.
58 J. R. Bleeke, R. R. Burch, C. L. Coulman and B. C. Schardt, *Inorg. Chem.*, 1981, **20**, 1316.
59 H. Werner, M. Schäfer, O. Nürnberg and J. Wolf, *Chem. Ber.*, 1994, **127**, 27.
60 O. Baron and P. Knochel, *Angew. Chem., Int. Ed.*, 2005, **44**, 3133; O. Baron and P. Knochel, *Angew. Chem.*, 2005, **117**, 3193.
61 S. Bontemps, L. Vendier and S. Sabo-Etienne, *Angew. Chem., Int. Ed.*, 2012, **51**, 1671; S. Bontemps, L. Vendier and S. Sabo-Etienne, *Angew. Chem.*, 2012, **124**, 1703.
62 J. Linshoeft, A. C. J. Heinrich, S. A. W. Segler, P. J. Gates and A. Staubitz, *Org. Lett.*, 2012, **14**, 5644.
63 M. Ahijado-Salomon, T. Braun and A. Penner, *Angew. Chem., Int. Ed.*, 2008, **47**, 8867; M. Ahijado-Salomon, T. Braun and A. Penner, *Angew. Chem.*, 2008, **120**, 8999.
64 M. D. Fryzuk, D. H. McConville and S. J. Rettig, *J. Organomet. Chem.*, 1993, **445**, 245.
65 J. K. MacDougall, M. C. Simpson and D. J. Cole-Hamilton, *Polyhedron*, 1993, **12**, 2877.
66 W. G. Henderson, M. J. How, G. R. Kennedy and E. F. Mooney, *Carbohydr. Res.*, 1973, **28**, 1.
67 D. Noveski, T. Braun, B. Neumann, A. Stammler and H.-G. Stammler, *Dalton Trans.*, 2004, 4106.
68 S. E. Boyd, L. D. Field, T. W. Hambley and M. G. Partridge, *Organometallics*, 1993, **12**, 1720.
69 M. Manger, J. Wolf, M. Teichert, D. Stalke and H. Werner, *Organometallics*, 1998, **17**, 3210.
70 W. S. Weston and D. J. Cole-Hamilton, *Inorg. Chim. Acta*, 1998, **280**, 99.

71 B. Xiao, Y.-M. Li, Z.-J. Liu, H.-Y. Yang and Y. Fu, *Chem. Commun.*, 2012, **48**, 4854.
72 H. R. Morales, H. Tlahuext, F. Santiesteban and R. Contreras, *Spectrochim. Acta*, 1984, **9**, 855.
73 H. F. Bettinger, M. Filthaus, H. Bornemann and I. M. Oppel, *Angew. Chem., Int. Ed.*, 2008, **47**, 4744; H. F. Bettinger, M. Filthaus, H. Bornemann and I. M. Oppel, *Angew. Chem.*, 2008, **120**, 4822.
74 F. A. Carey and R. J. Sundberg, *Organische Chemie*, *Ein weiterführendes Lehrbuch*, VCH Verlagsgesellschaft GmbH, Weinheim, 1995.
75 F. H. Allen, O. Kennard, D. G. Watson, L. Brammer, A. G. Orpen and R. Taylor, *J. Chem. Soc., Perkin Trans. 2*, 1987, S1.
76 P. Zhao and J. F. Hartwig, *J. Am. Chem. Soc.*, 2005, **127**, 11618.
77 T. Braun, D. Noveski, B. Neumann and H.-G. Stammler, *Angew. Chem., Int. Ed.*, 2002, **41**, 2745; T. Braun, D. Noveski, B. Neumann and H.-G. Stammler, *Angew. Chem.*, 2002, **114**, 2870.
78 J. R. Bleeke and A. J. Donaldson, *Organometallics*, 1988, **7**, 1588.
79 M. E. Fasulo, E. Calimano, J. M. Buchanan and T. D. Tilley, *Organometallics*, 2013, **32**, 1016.
80 P. Zhao, C. D. Incarvito and J. F. Hartwig, *J. Am. Chem. Soc.*, 2007, **129**, 1876.
81 M. A. Beenen, C. An and J. A. Ellman, *J. Am. Chem. Soc.*, 2008, **130**, 6910.
82 K. Hong and J. P. Morken, *J. Am. Chem. Soc.*, 2013, **135**, 9252.
83 C. Solé, H. Gulyás and E. Fernández, *Chem. Commun.*, 2012, **48**, 3769.
84 S.-S. Zhang, Y.-S. Zhao, P. Tian and G.-Q. Lin, *Synlett*, 2013, 437.
85 T. Braun and F. Wehmeier, *Eur. J. Inorg. Chem.*, 2011, 613.
86 H. Amii and K. Uneyama, *Chem. Rev.*, 2009, **109**, 2119.
87 J. L. Kiplinger, T. G. Richmond and C. E. Osterberg, *Chem. Rev.*, 1994, **94**, 373.
88 M. F. Kuehnel, D. Lentz and T. Braun, *Angew. Chem., Int. Ed.*, 2013, **52**, 3328; M. F. Kuehnel, D. Lentz and T. Braun, *Angew. Chem.*, 2013, **125**, 3412.
89 S. Erhardt and S. A. Macgregor, *J. Am. Chem. Soc.*, 2008, **130**, 15490.
90 A. L. Raza, J. Panetier, M. Teltewskoi, S. A. Macgregor and T. Braun, *Organometallics*, 2013, **32**, 3795.
91 A. Nova, S. Erhardt, N. A. Jasim, R. N. Perutz, S. A. Macgregor, J. E. McGrady and A. C. Whitwood, *J. Am. Chem. Soc.*, 2008, **130**, 15499.
92 A. Nova, M. Reinhold, R. N. Perutz, S. A. Macgregor and J. E. McGrady, *Organometallics*, 2010, **29**, 1824.
93 E. Q. Jiao, F. T. Xia and H. Zhu, *Comput. Theor. Chem.*, 2011, **965**, 92.
94 E. Clot, O. Eisenstein, N. Jasim, S. A. Macgregor, J. E. McGrady and R. N. Perutz, *Acc. Chem. Res.*, 2011, **44**, 333.
95 V. V. Grushin, *Acc. Chem. Res.*, 2010, **43**, 160.
96 M. D. Fryzuk and W. E. Piers, *Organometallics*, 1990, **9**, 986.
97 H. Braunschweig, M. Burzler, K. Radacki and F. Seeler, *Angew. Chem., Int. Ed.*, 2007, **46**, 8071; H. Braunschweig, M. Burzler, K. Radacki and F. Seeler, *Angew. Chem.*, 2007, **119**, 8217.
98 M. Higuchi and K. Yamamoto, *Polym. Adv. Technol.*, 2002, **13**, 765.
99 W. Dei, R. Srinivasan and J. A. Katzenellenbogen, *J. Org. Chem.*, 1989, **54**, 2204.
100 L. Liu, S. Zhang, X. Fu and C.-H. Yan, *Chem. Commun.*, 2011, **47**, 10148.
101 G. M. Sheldrick, *Acta Crystallogr., Sect. A: Fundam. Crystallogr.*, 2008, **64**, 112.
102 G. M. Sheldrick, *SHELXL, Crystal Structure Refinement*, University of Göttingen, Germany, 2013.
103 A. Altomare, M. C. Burla, M. Camalli, G. L. Cascarano, C. Giacovazzo, A. Guagliardi, A. G. G. Moliterni, G. Polidori and G. R. Spagna, *J. Appl. Crystallogr.*, 1999, **32**, 115.